(NASA-CR-158241) CHEMICAL VAPOR DEPOSITION OF HIGH T SUB c SUPERCONDUCTORS Final Report, 1 May 1975 - 31 Dec. 1978 (California Univ., San Diego, La Jolla.) 60 p HC A04/MF A01 CSCL 07D G3/25

N79-19113

Unclas 16417

FINAL REPORT

Chemical Vapor Deposition of High T_c Superconductors

Principal Investigators

G. W. Webb
and
John J. Engelhardt

NASA GRANT NASA/L/NSG-3055

Effective Dates: May 1, 1975 through December 31, 1978

University of California, San Diego
Institute for Pure and Applied Physical Sciences
La Jolla, California 92093

UNIVERSITY OF CALIFORNIA, SAN DIEGO

BERKELEY • DAVIS • IRVINE • LOS ANGELES • RIVERSIDE • SAN DIEGO • SAN FRANCISCO • SANTA BARBARA • SANTA CRUZ

INSTITUTE FOR PURE AND
APPLIED PHYSICAL SCIENCES

LA JOLLA, CALIFORNIA 92093

March 29, 1979

NASA Scientific & Technical Information
P. O. Box 8757
Baltimore/Washington International Airport
Baltimore, Maryland 21240

Gentlemen:

Please find enclosed two copies of our final report on NASA Grant NSG-3055. Please do not hesitate to contact me about any question that may arise.

Yours truly,

George W. Webb

George W. Webb

Table of Contents

		Page
	Summary	1
I.	Introduction	2
II.	CVD Apparatus	3
III.	Measurement Details	10
IV.	Systems Investigated	12
V.	Effect of Substrate Materials and Annealing on CVD Films	30
VI.	Critical Fields and Current Densities	36
VII.	Conclusions and Recommendations	40
VIII.	References	41
IX.	Publications of Research Supported in Part or Totally by this Grant	43

Summary

This report describes the results of an investigation into the synthesis and properties of high temperature superconducting materials. A chemical vapor deposition apparatus was designed and built which is suitable for the preparation of multicomponent metal films. This apparatus was used to prepare a series of high T_c A-15 structure superconducting films in the binary system Nb-Ge. The effect on T_c of a variety of substrate materials was investigated. An extensive series of ternary alloys were prepared with the approximate composition $Nb_3Ge_{1-x}"B"_x$ where "B" = Sn, Ga, Si and As. The influence of "B" on T_c, on the critical current density, J_c, and on the upper critical field H_{c2} was examined. No increase in T_c was observed but modest increases in J_c and H_{c2} were found for Ga, which, however, have not exceeded the maximum values observed in binary NbGe prepared by other techniques.

Conditions allowing the brittle high T_c ($\simeq$ 18 K) A-15 structure superconductor Nb_3Al to be prepared in a low T_c but ductile form were found. Some of the ways that the ductile (bcc) form can be cold worked or machined are described. Measurements of rate of transformation of cold worked bcc material to the high T_c A-15 structure with low temperature annealing are given. Preliminary measurements indicate that this material has attractive high field critical current densities.

I. Introduction

This research program was designed to investigate the conditions necessary for the preparation of superconducting materials with properties superior to those known at present. Properties of interest to use are the superconducting critical temperature (T_c), critical magnetic field strength (H_{c2}), and critical current density (J_c). We have focused our attention on the niobium based A-15 structure materials for this study. This class of materials exhibits the highest known transition temperature, $T_c = 23$ K, high critical magnetic field strengths $H_{c2} \simeq 400$ kG and very high critical current densities, $J_c > 10^6$ a/cm^2. With properties of this magnitude, it is clear that for many applications, a tradeoff of properties will be acceptable, for example, higher critical currents at the expense of lower critical temperatures.

The sample preparation technique we have adopted is that of chemical vapor deposition, one which has been used widely in the semiconductor industry and has even been used for the commercial production of practical superconducting materials. Among the advantages of the technique are high growth rates, $\sim 1/3$ μ/min in the present case, low turn around time for preparing new samples and the ability to synthesize material at low temperature, e.g., $T_{deposition} \leq 1000°C$. Low temperature synthesis is essential for the preparation of several high T_c materials which are unstable with respect to other, lower T_c, phases. That these high T_c phases form at all is due to their having more favorable growth kinetics at the (low) deposition temperatures.

Interest in pseudobinary systems have grown out of our investigation into preparation of high T_c Nb_3Ge, the material with the highest known T_c. The specimens prepared have been characterized through measurement of the overall composition of the deposited film by x-ray spectrographic analysis. X-ray diffraction was used to ascertain phase relations in the systems. Superconducting properties were characterized by measurement of the transition temperature and in selected cases measurements were made of the critical magnetic

field and of the critical current density.. As Nb_3Ge has the highest known transition temperature, a large part of our investigation has been the replacement of part of the Ge in this material with other elements. We have investigated the following systems: $Nb_3(Ge_{1-x}"B"_x)$ with "B" = Sn, Ga, As, Si, Sb, P, Au, Pt, Cu, Fe, O. On the basis of the results obtained, we have concentrated on Sn, Ga, As, and Si.

II. CVD Apparatus

Good quality films of the high temperature superconductor Nb_3Ge have been synthesized by the method of chemical vapor deposition (CVD).[1] Ribbons of the high T_c superconductor Nb_3Sn are available commercially based on the CVD method developed by Hanak.[2] The CVD method has the advantage of relatively high deposition rates ($\sim$ 1 μ/min) and the capability of producing thick uniform films without elaborate apparatus. In order to study the effects of other elements on the superconductivity of Nb_3Ge, an apparatus was needed in which it was simple to change elements and to transport simultaneously a number of different elements. In a typical CVD apparatus it is necessary to have a separate source, flowmeter and flow control for each element. With the apparatus described here, these requirements are reduced and the transport of multicomponent compounds is simplified. The films thus produced have uniform overall compositions in depth because of the inherent close control over the ratios of metal chloride densities in the transport stream as the film is deposited. Also the films have a very static composition gradient down the length of the deposition zone with a uniform composition across the zone. This was found to result from the highly turbulent flow pattern existing in the reduction-deposition zone which encourages rapid mixing of the chlorides with hydrogen. A number of mixing configurations were tried and the system described here was chosen because it satisfied two criteria for Nb-Ge films: (1) minimization of the Nb_5Ge_3 phase, (2) well- resolved $\alpha_1 \alpha_2$ doublets for high angle lines {611} in the x-ray diffraction patterns.

---

†Based on a paper submitted to J. Appl. Phys.

The reaction zone of the apparatus is shown in Fig. 1. Except for the ingot and substrates everything shown is fabricated of fused quartz. A quartz tube envelope (~ 3 cm dia.) passes through three tube furnaces of length 20 cm each. A precast ingot of uniform overall composition is situated in the left-hand furnace at approximately 700°C. A gas stream of chlorine and He carrier passes through a nozzle, impinging upon and reacting with the ingot, producing a gaseous mixture of chlorides of the metals in the ingot. It is found that the chlorine jet bores an even hole in the ingot and leaves very little condensed chlorides behind. Thus the gaseous metal chloride stream produced has a composition ratio of metals closely approximating that of the ingot, and is automatically quite constant at least to the extent of overall homogeneity of the ingot.

The chlorides are then passed through a nozzle in the second furnace inclined at $\sim 45°$ to the axis of the quartz envelope. This jet intersects with a high velocity jet of hydrogen parallel to and at the axis of the envelope. These two quartz nozzles were aligned precisely such that the two jets intersect exactly. This was accomplished by mounting the two tubes in an adjustable jig; passing water through both nozzles under pressure and positioning them for best interaction. The two tubes were then permanently fused together with quartz rods.

The jets issuing from both nozzles were of such high velocity as to become immediately turbulent and thus the chlorides and hydrogen mixed very rapidly. The hydrogen nozzle was bent downward slightly to compensate for the deflection due to the chloride jet. The gases are then swept into the third (high temperature) furnace where reduction and deposition takes place. A number of substrates are distributed in this zone. A small flow of He was fed into each end of the quartz envelope in order to isolate room temperature metallic end caps from the reactants.

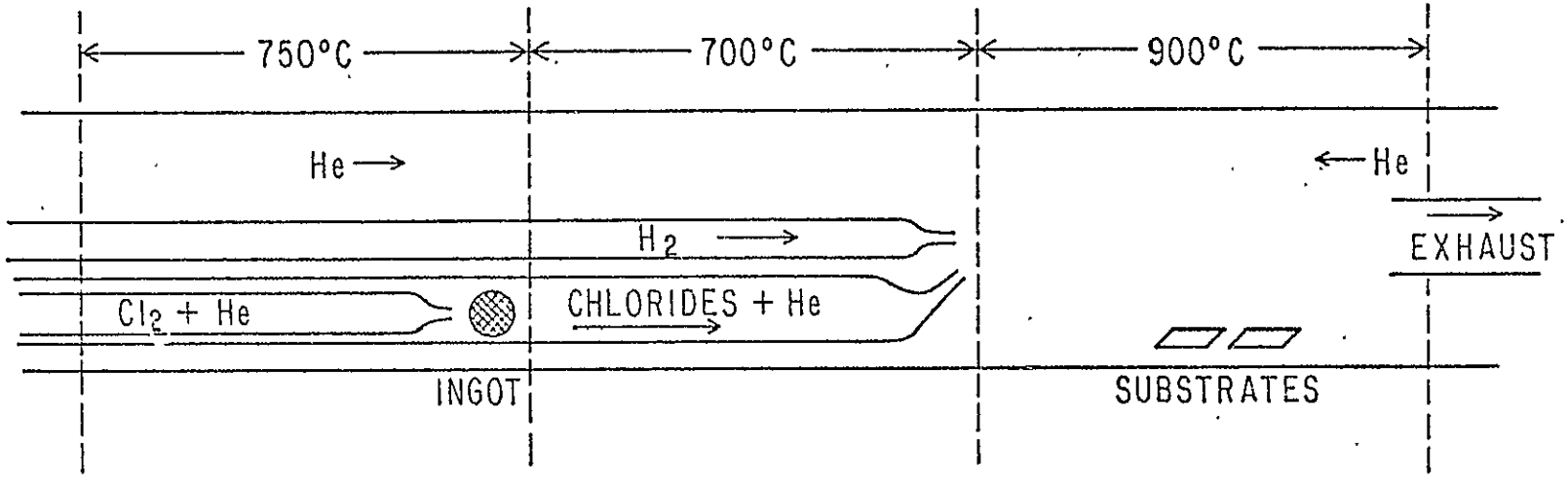

Fig. 1. Reaction zone of the chemical vapor deposition apparatus.

As an example of typical operating conditions, for the deposition of Nb_3Ge or Nb_3Sn operational parameters are as follows:

Nozzle diameters

Cl_2	0.25 mm
H_2	0.25 mm
Chloride	0.5 mm

Flow rates

Cl_2	17 ml/min
He (with Cl_2)	29 ml/min
H_2	750 ml/min
Ingot weight ~	1 gram

For a typical run of 15 minutes, deposits were in the range of 5 to 10 μ thick. Thickness and composition were the most uniform in positions from about 9 to 16 cm into the 20 cm deposition furnace with the niobium content of the deposits gradually increasing downstream. Generally the niobium content was about 1 atomic percent greater at position 12.5 cm than at position 10 cm.

As expected, it is found that the composition of the deposits does not always equal that of the ingots. This deviation occurs in the reduction-deposition part of the process. The reduction efficiency is dependent in part on the free energies of formation of the metal chlorides in relation to that of HCl and, in practice is often significantly less than 100%. Thus the deposit composition is a function of these free energies besides being dependent upon the ingot composition. However, the deposit composition does depend monotonically on the ingot composition. An example of the type of relationship found between ingot and deposit composition can be seen in Fig. 2 for the case of Nb-Sn and Nb-Ge transport. Deposit compositions were determined with an electron microprobe with an accuracy of ±1 atomic percent. The relative stability of the intermediate phases clearly influences

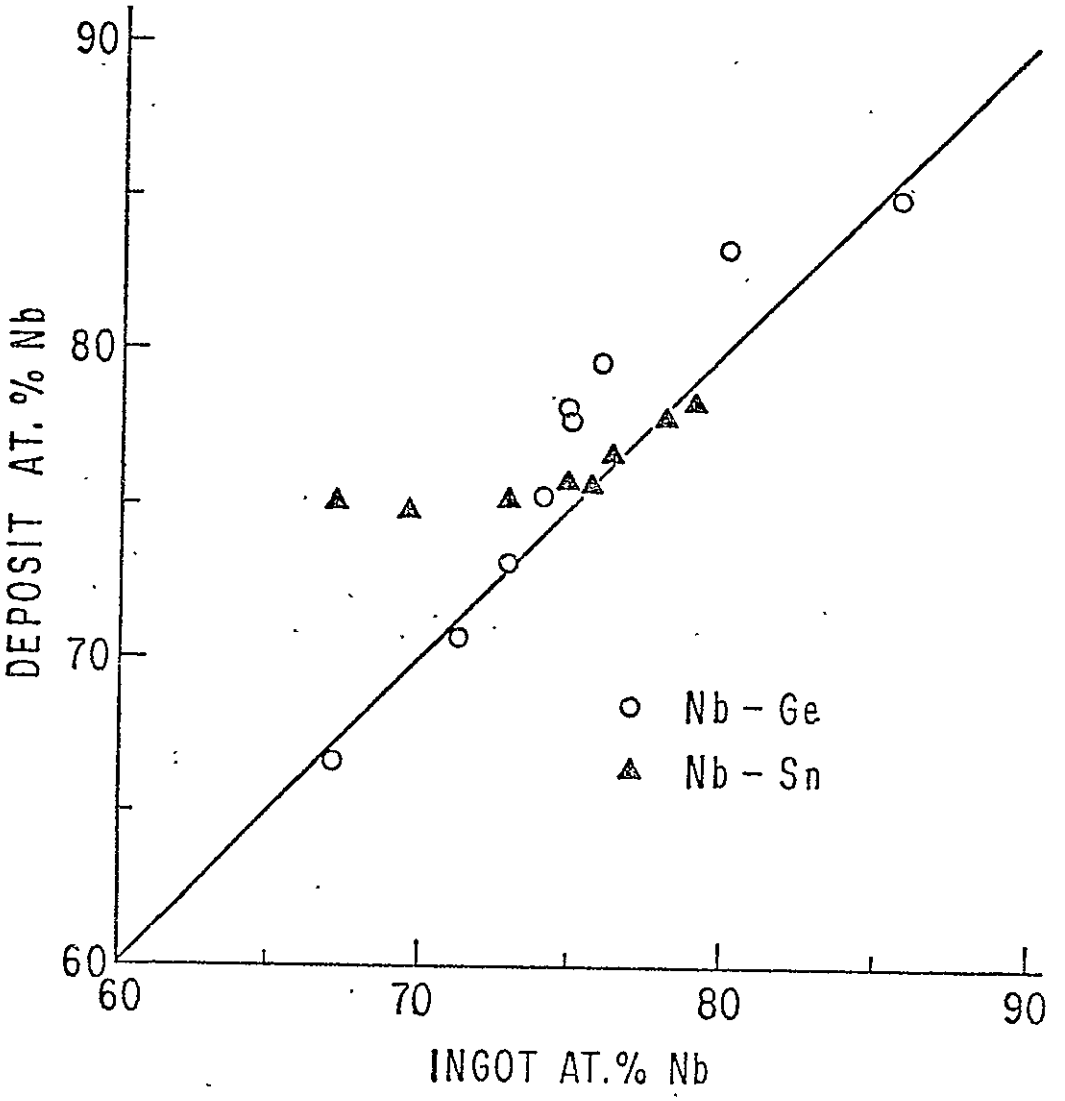

Fig. 2. CVD deposit composition versus ingot composition for transport of the binary system Nb-Sn and Nb-Ge.

the deposit composition. In the Nb-Sn case there is no indication of Nb_6Sn_5 in the deposits even when the ingot is quite Nb-poor. The inability of producing films of A-15 Nb-Sn with Nb less than 75 at. % by CVD has been reported before.[2] For the Nb-Ge case an ingot with Nb composition less than ~ 75 at. % produces deposits containing Nb_5Ge_3.

As an example of the degree of homogeneity of the deposits obtained by this method, the strong $\alpha_1\alpha_2$ splitting of the A-15 {611} lines of Nb-Sn and Nb-Ge samples can be seen in Fig. 3. Both of these deposits were approximately 5 μm thick and were measured in a diffractometer while still on their alumina substrates. The Nb-Ge diffraction pattern showed very strong A-15 lines and very weak Nb_5Ge_3 lines and the Nb-Sn had only A-15 lines.

The superconducting transition temperatures as measured by 4-probe resistivity are, for the Nb-Sn and Nb-Ge samples in Fig. 3, respectively: Onset temperature, 17.8 and 21.9 °K, transition midpoint, 17.6 and 20.7 °K, and transition widths (10 to 90%) 0.1 and 0.8 °K.

We have successfully deposited some binary and ternary alloys composed of members of the following series of elements: Nb, Ta, Ge, Sn, Ga, Si, As, P, Sb, Cu, and Fe. As examples of extremes in transportability; Nb, Ta, Ge and Sn transported easily whereas Ga and Si required large excesses in the ingots due to the high stability of their chlorides. Au on the other hand, would not transport with niobium in any significant quantity because of the low relative stability of gold chloride. Additional elements that are likely to co-transport with the elements given above are: Co, Ni, Bi and possibly, Mn, Cu, Ag, B and In.

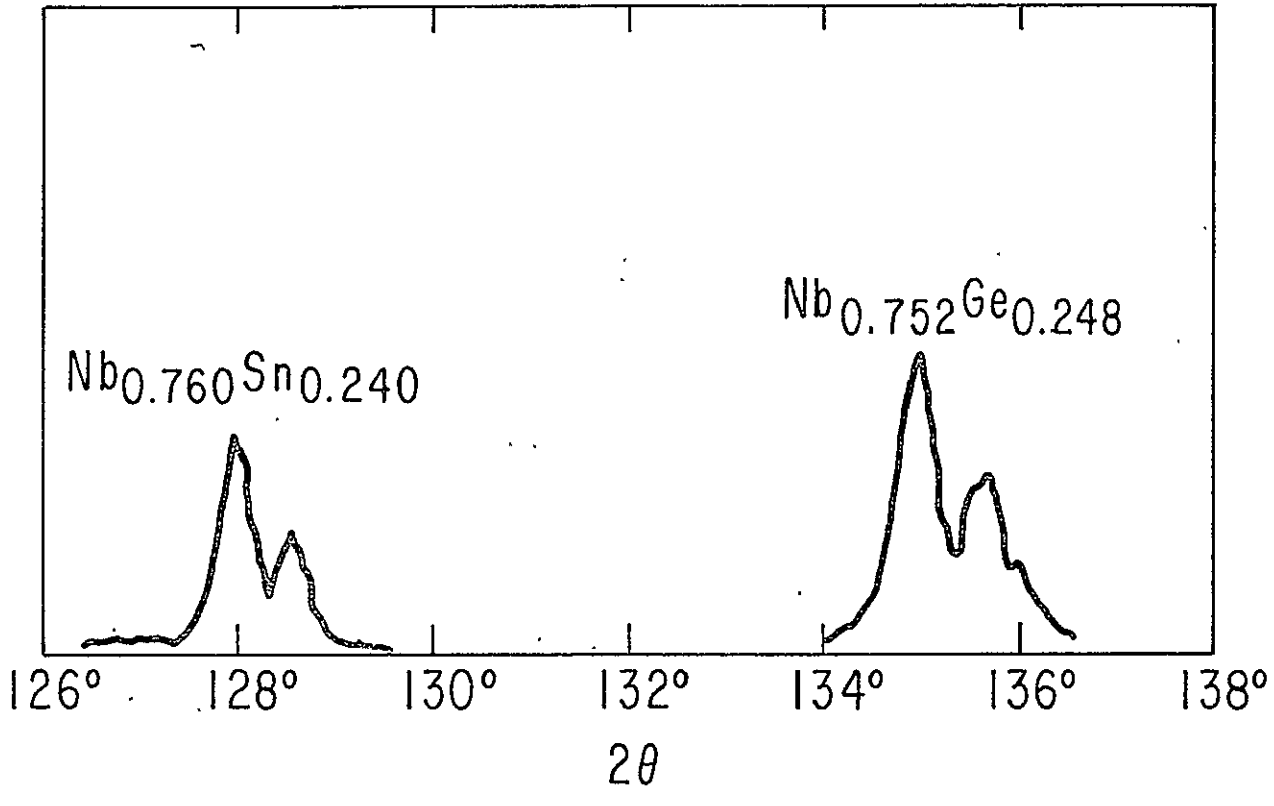

Fig. 3

III. Measurement Details

A. X-ray Chemical Analysis and Impurity Estimates

To determine accurately the composition of thin films, the method of choice is the electron microprobe with the careful use of accurate calibration standards. The scanning electron microscope (SEM) available to us here has the necessary x-ray detector and electronics to serve as a microprobe. We found that two modifications were necessary to achieve sufficient accuracy in the chemical analysis. One was to build a holder for the films and standards for reproducible positioning in the SEM. The other was to correct for the large fluctuations found in the SEM electron beam current used for x-ray excitation. This was resolved by rotating a "chopper" made of titanium just over the sample in the electron beam. The essential purpose of this "chopper" is to interpose in the electron beam a piece of Ti, thereby producing the Ti x-ray, for a reproducible fraction of the counting time. The Ti x-ray count integrated over the counting period is then proportional to the integrated electron current and can be used to normalize the measurements. The electron beam potential employed was 17.5 kV. The area scanned was in the form of a square raster of dimensions 0.5 mm × 0.5 mm. The accuracy of this system was then determined by measuring 5 binary and ternary samples of known composition. The result was that the measured composition of the standards fell within ±1% of the known which is considered to be sufficient accuracy for the purposes of this project at the present time.

There has been discussion in the literature whether the high T_c A-15 phase in the Nb-Ge system at the stoichiometric composition is impurity stabilized.[3] Several reports have stated that either air or oxygen alone had to be admitted into the system, e.g. co-evaporation systems or sputtering systems before high T_c films could be prepared.[3,4] [If actually true the role the impurity plays might be through the kinetics of growth rather than altering thermodynamics in the system.] It is not possible to detect oxygen in

small amounts with the analytical tools available to us at the present time. However, we did find a rather satisfactory method. To do this, we deposited by CVD a "pure" 4 μ Nb film under conditions otherwise identical to those successful for growing high T_c Nb_3Ge films. It is known[5] that interstitial oxygen in the dilute limit contributes residual resistivity to Nb at the rate $\Delta\rho/\Delta c \simeq 4.5 \times 10^{-10}$ Ω cm per at. ppm O. Almost identical incremental resistivity values are quoted for C and N. The measured residual resistance ratio of our Nb film was $R(300\ K)/R(T_c) = 10$ which yields a residual resistivity of 1.5 μ Ω cm and an upper bound to the oxygen concentration for example of 0.35 at.% O. (Note that Nb can dissolve more O than this.[6]) This is in upper bound because it ignores other contributions to the residual resistivity due to grain boundaries, etc. Our starting material is electron beam melted, cold rolled, Nb sheet with a resistance ratio of 24.[7] Attributing all of the residual resistance of the starting material to O yields an oxygen content of 0.15 at.% (1500 ppm) about a factor of two higher than typical analyses for material of this type. Thus it is felt that no more than 0.2 at.% impurity total for O, C, and N have been added in the CVD process.

The phases present in the films and their lattice parameters were measured with the films on the substrates by x-ray diffraction using CuKα radiation and a graphite monochromator. Oriented growth was clearly evident in many of the films. The x-ray diffraction patterns of the films exhibited resolved doublets for the {611} lines except where noted.

Superconducting transition temperatures were determined by 4-probe alternating current resistance measurement usually at 200 Hz. The samples, on their alumina substrates, were of a few millimeter dimensions. Electrical contact was made by ultrasonic soldering of platinum leads onto the films with indium solder. The characteristic superconducting transition temperature used was the midpoint of the resistive transition (T_m). A measure of the transition width was taken to be the difference in temperature between the 10 and 90% points of the resistive transition. The current density varied but was always in the low current density limit.

IV. Systems Investigated

A major goal of this research program was to investigate the effect of third element substitutions for Ge in $Nb_{\sim 3}Ge$ on the superconducting properties, especially T_c and H_{c2}. Also of interest were the effect of such substitutions on metallurgical parameters such as stoichiometry with respect to Nb content in the A-15 phase, lattice parameters and the precipitation of additional phases.

For chemical and metallurgical reasons, the elements chosen for alloy studies are neighbors of Ge in the periodic table as shown in Fig. 4. As can be seen Si and Sn are isovalent with Ge while Ga and As have valences differing by one from Ge. It is now well known[8] that A-15 phases exist over a range of compositions and that T_c is highest, as in the case of $Nb_{\sim 3}Ge$, when the composition is near stoichiometry (3 : 1). Accordingly, special emphasis was placed on maintaining stoichiometry with respect to Nb in the ternary alloys. Stoichiometry is schematically represented by the 75% line in Nb corner of the ternary diagram of Fig. 4.

For the sake of comparison a complete set of binary $Nb_{\sim 3}Ge$ specimens of different composition were prepared by CVD. Then under identical conditions a series of ternary alloys were prepared of the form $Nb_{\sim 3}Ge_{1-x}"B"_x$ where "B" = Ga, Sn, As, Si and the amount is generally less than 1. Only in the favorable case of Sn could the whole range $0 \leq x \leq 1$ be covered.

A series of binary Nb-Ge alloys was first synthesized to serve as a basis for comparison with the ternaries. The effect of composition on the lattice parameter (a_o) and on the superconducting transition temperature (T_c) are shown. Here T_c represents the midpoint of the superconducting transition as measured by 4-probe resistance. Errors are: for the composition, ±1 at.%, for a_o ± 0.001 Å and the transition temperature widths were typically in the range 0.3 to 1.5°K.

$Nb_{\sim 3} Ge_{1-a} X_a$

X = Sn , As , Ga , Si

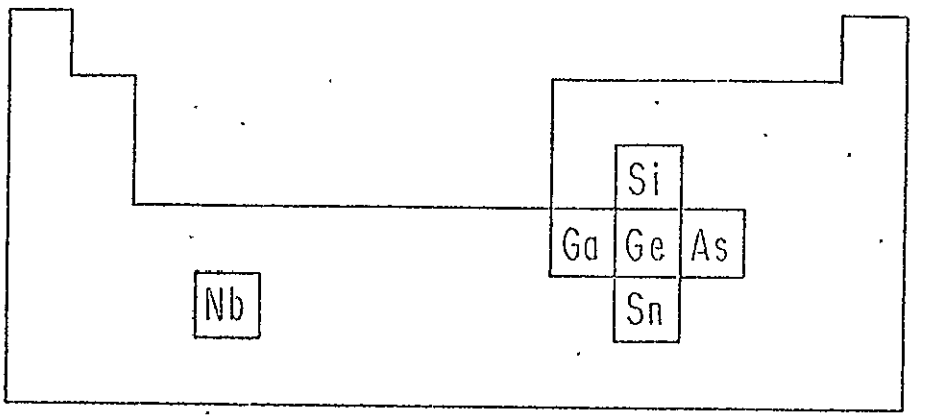

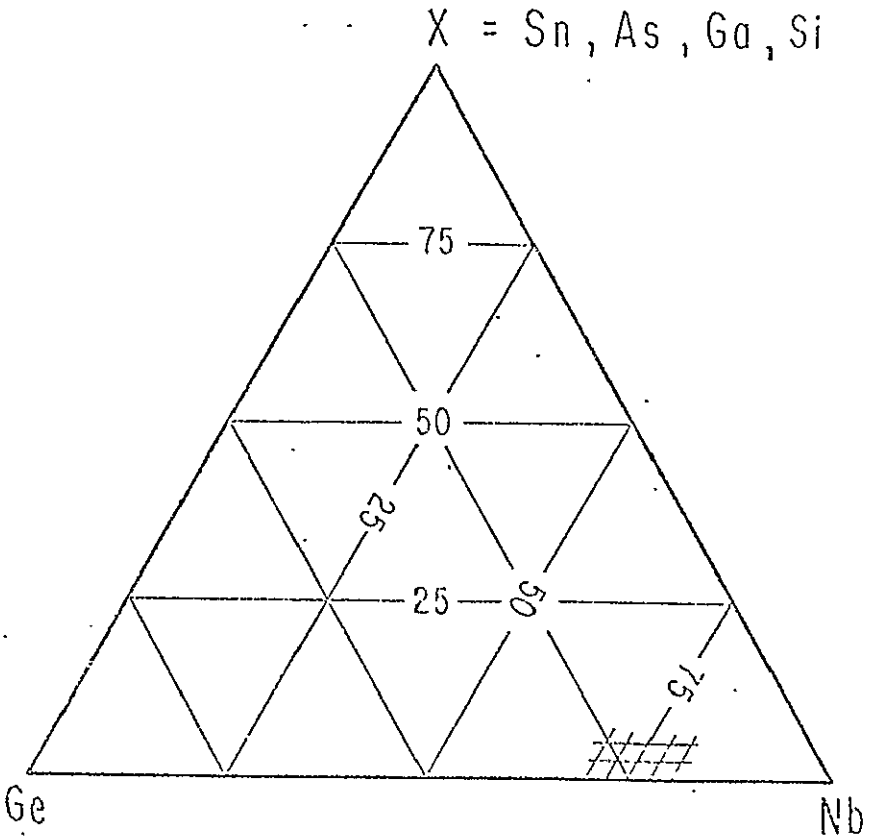

Fig. 4

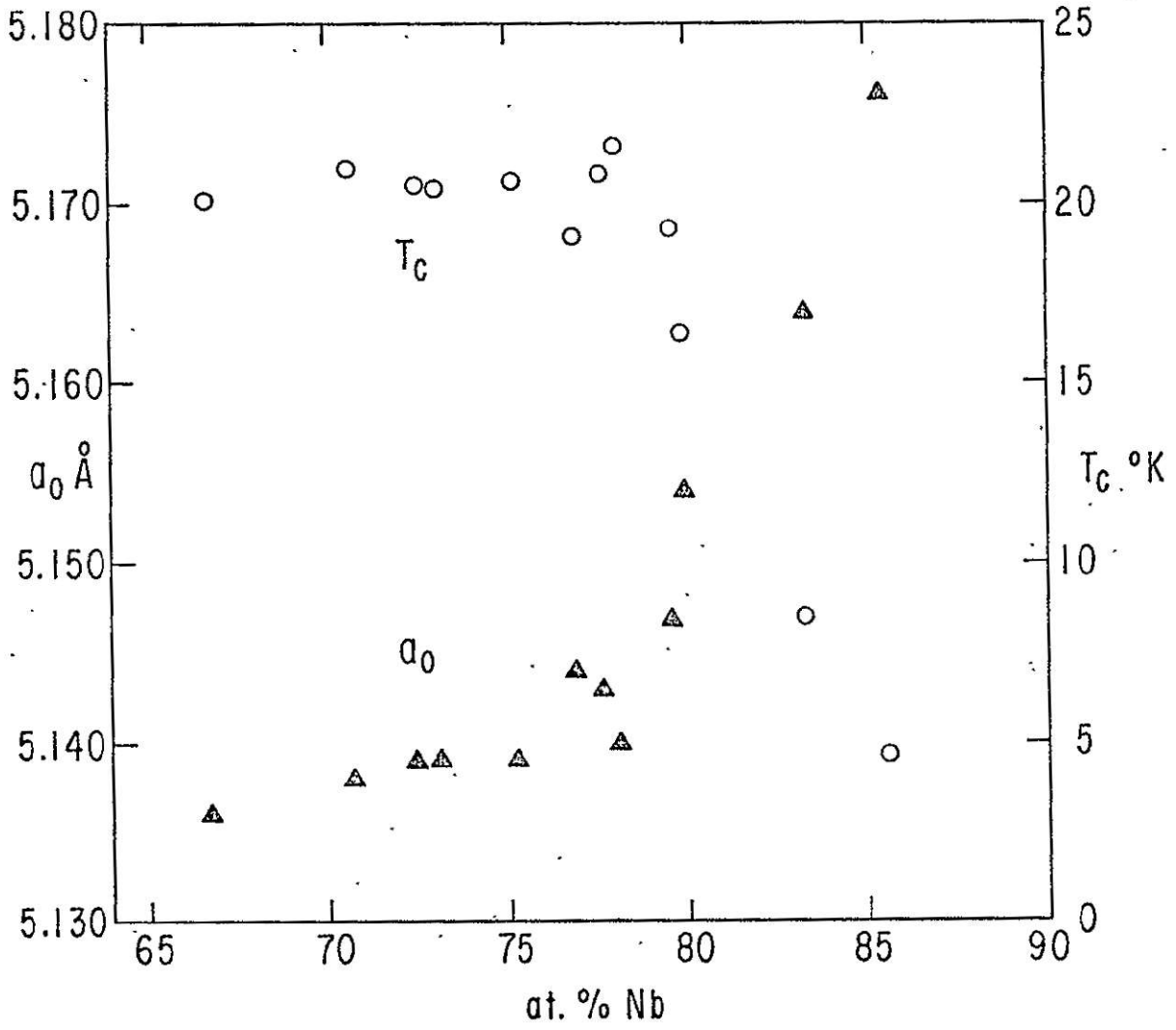
5.180
5.170
5.160
5.150
5.140
5.130
a_0 Å
25
20
15
10
5
0
T_c °K
T_c
a_0
65
70
75
80
85
90
at. % Nb

Fig. 5

Starting with the Nb-rich side the well-known decrease in lattice parameter for A-15 Nb-Ge is seen as stoichiometry is approached and less Ge sites are occupied by the excess Nb. The change in a_o is due to the substitution of Ge atoms of smaller radius (R^B_{Ge}) on the "B" sites in A-15 "A_3B" for the larger Nb atoms of radius R^B_{Nb}. As the measured overall composition of the deposit approach 75 at. % Nb from the Nb rich side, there is a gradual increase in the amount of Nb_5Ge_3, "σ" phase, observed in the diffraction patterns of the films. Then for overall Nb concentrations less than 75 at. % the A-15 lattice parameter remains nearly constant, indicating a nearly constant composition in the A-15 phase. Coincident with this (nearly) unchanging A-15 lattice parameter is an observed increase in the amount of "σ" phase. At 65 at. % Nb we find that the A-15 phase is no longer present. This situation is quite similar to that of crossing and equilibrium phase boundary into a two phase region, although these materials are not in thermodynamic equilibrium.

A. NbGeSn system*

Introduction

The compound Nb_3Sn has been the subject of considerable investigation since its discovery in 1954 by Matthias, Geballe, Geller and Corenzwit.[9] For about 15 years after its discovery, it was the highest transition temperature (T_c) superconductor known with T_c = 18 K. During this time the conditions necessary for the preparation of material in forms suitable for practical application were under intensive study. These efforts were successful in developing Nb_3Sn as a technologically useful material.

In 1956 Carpenter and Searcy discovered[10] that the compound Nb_3Ge had the A-15 structure also. Soon thereafter, Geller[11] pointed out that

---

*The section on NbGeSn system has been published in J. Less Common Metals 62, 89 (1978).

given reasonable metallic radii the observed lattice parameter was too large, suggesting that the material was Nb rich with respect to stoichiometry. Later it was reported[12] that the equilibrium homogeneity range for the A-15 phase did not include the stoichiometric composition, extending from about $Nb_{0.87}Ge_{0.13}$ to only $Nb_{0.82}Ge_{0.18}$ at 1600°C. The observed T_c's were reported in the range 5 K to 7 K for such material prepared by more or less equilibrium techniques. In 1965 Matthias et al. reported[13] that non-equilibrium "Nb_3Ge" prepared by splat cooling showed the onset of a superconducting transition at 17 K. The higher T_c onset they attributed to non-equilibrium A-15 structure material closer to the stoichiometric composition.

There have been a number of investigations into pseudobinary alloys formed between Nb_3Sn and off stoichiometric "Nb_3Ge." At the time these studies were carried out because of interest in the high T_c of Nb_3Sn. Hagner and Saur[14] measuring sintered samples, found T_c to drop in the neighborhood of Nb_3Sn with the addition of Ge. Likewise with sintered samples, Galasso et al.[15] found that T_c varied approximately linearly between Nb_3Sn (17.8 K) and Nb_3Ge (6 K). Alekseevskii et al.[16] found, for levitation melted samples, that T_c followed a smooth curve, sloping downward at 18.1 K at Nb_3Sn and leveling out to 7.1 K at Nb_3Ge. Otto[17] found a slight maximum in T_c near Nb_3Sn for arc-melted, annealed samples with the addition of Ge. They also found a linear change (Vegard's law) in the lattice parameter between Nb_3Sn and "Nb_3Ge."

More recently, Gavaler[18] has shown that nonequilibrium Nb_3Ge can be sputtered onto heated substrates with T_c over 22 K. This result clearly indicates the need for a re-measurement of the Nb-Ge-Sn A-15 system.

Following Gavaler's discovery, it was shown[1] that high T_c Nb_3Ge could be made by the method of chemical vapor deposition (CVD) via chlorides onto substrates in the same range of temperatures, 700°C to 950°C employed in the sputtering investigation. The CVD method

was originally applied by Hanak[2] to prepare Nb_3Sn in the same temperature range. As the conditions for deposition of both compounds are similar, this method was chosen for the ternary system and the results are reported here.

Results

A series of specimens were prepared in the Nb rich corner of the ternary system. A variety of substrates were employed. These included alumina, sapphire, Nb, Mo, beryllia, copper and lithium niobate. Alumina proved to be a very good thermal expansion match for samples near the composition Nb_3Ge and to put Nb_3Sn alloys under slight tension when cooled.

Under the present experimental conditions we observed no evidence that A-15 structure alloys could be prepared with less than the stoichiometric amount of Nb. On the NbGe side of the ternary system it was found that as the measured Nb content went from the Nb rich to the Nb deficient side of stoichiometry there was a gradual increase in the amount of Nb_5Ge_3 co-deposited with the A-15 phase. For NbSn alloys, even with gas compositions rich in Sn, the most Sn rich deposits were found to be single phase A-15 structure having a measured composition of Nb_3Sn. This behavior in the NbSn system has been noted earlier by Hanak.[2]

Figure 6 shows some data taken from pseudobinary alloys with approximately fixed Nb content of 76 at. %. It was necessary to include data from samples with a measured Nb content in the band 76 at. % $^{+0.9}_{-0.8}$. In part a) of the figure the T_c midpoint is plotted versus composition expressed as the ratio of Sn to Ge+Sn. The broad minimum in T_c midpoint is easily seen.

In part b) of Fig. 6 we have plotted resistance ratio, $\Gamma = R(300\ K)/R(T_c)$, versus composition. Extrapolating the data to 0 K so as to obtain R(300 K)/R(0 K) gives a negligible ($< 6\%$) change in the qualitative features of the data. The chief such feature of these data is a broad minimum of Γ similar to that in T_c.

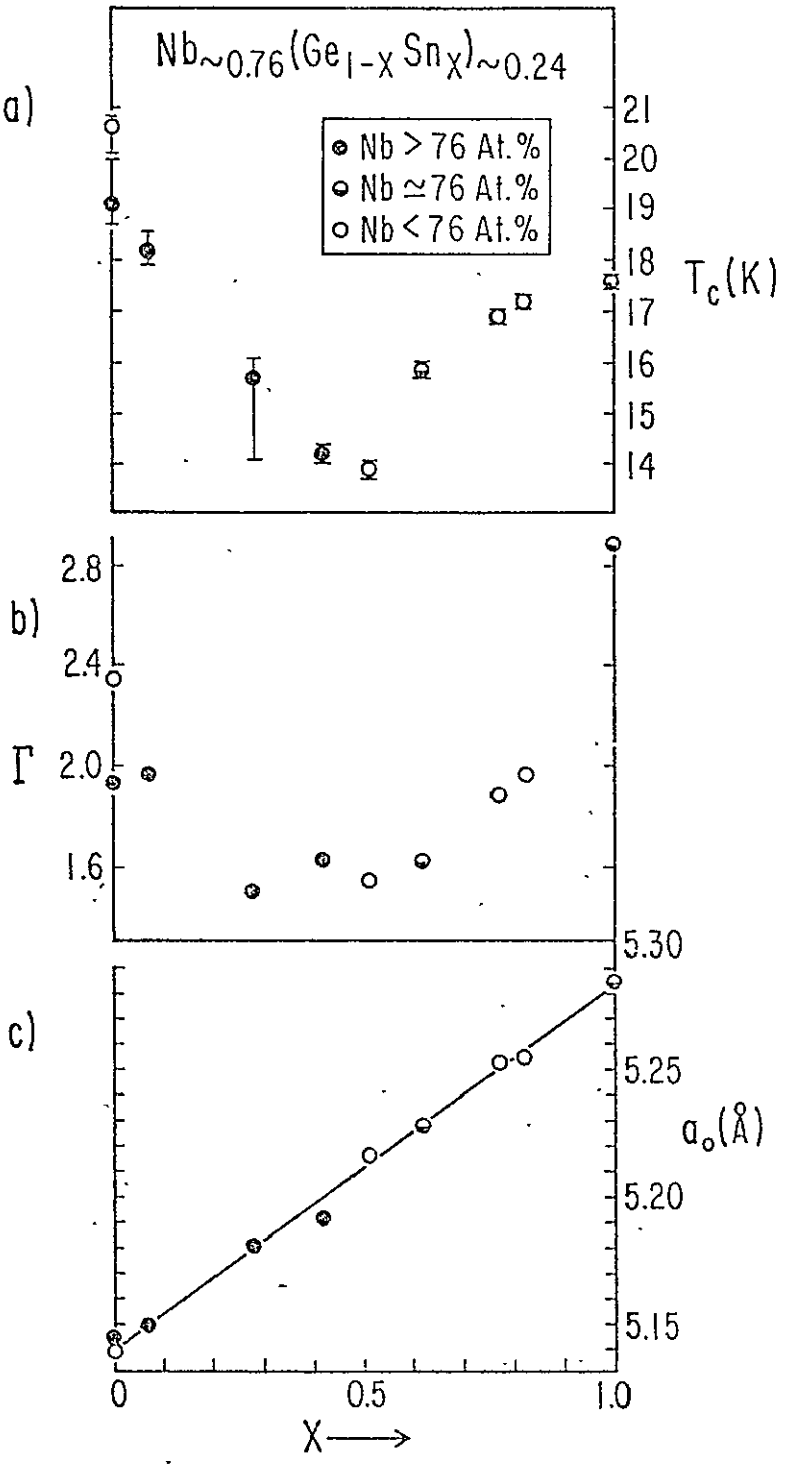

Fig. 6. Superconducting transition temperature (T_c), resistance ratio (Γ) and lattice parameter (a_o) variation with fraction (x) of Sn across the Nb-Ge-Sn system. The transition widths on the T_c points represent temperatures of 10 and 90% of the transitions.

In part c) of Fig. 6 we have plotted the measured mean A-15 lattice parameters of the deposits on alumina substrates. Comparison with deposits on very thin (5μ) Nb substrates suggests that the lattice parameter is negligibly affected by differential thermal contraction for NbGe binary samples and that for NbSn binary alloys the lattice parameter is about 0.003 Å smaller because of stress. The diffraction patterns from which the lattice parameters were calculated contained second phase lines only for Ge rich compositions. These additional lines were of very weak intensity. For the binary end points the high angle A-15 diffraction lines displayed very well split $\alpha_1 \alpha_2$ doublets. Toward the middle of the system, however, there was a clear broadening of the high angle lines. Figure 7 is a tracing of representative x-ray patterns showing these effects for the {611} lines.

Figure 8 shows lattice parameter and T_c midpoint results near the NbGe edge of the ternary diagram. It is evident that proceeding upward along constant Nb lines there is an (expected) increase in the A-15 lattice parameter as Sn replaces Ge. Coincident with Sn replacement of Ge there is a decrease in T_c, similar to that shown in Fig. 6 for 76 at. % Nb.

Discussion

There are two qualitative features of the data which can be discussed. The first is the depression of T_c over the entire range of pseudobinary compositions in Fig. 6 and the accompanying minimum in resistance ratio. The second is the presence of the x-ray line broadening for compositions near $x \sim 0.5$ as shown in Fig. 7.

Nb base high T_c A-15 structure compounds display a maximum of T_c at or near stoichiometry with T_c having a strong dependence on composition, being depressed with an average slope of -1 to -2.5 K/at. % when there is excess Nb.[8] (For the case of $Nb_{3+x}Al$ the T_c has been reported[19] to have a broad maximum near stoichiometry.) When there is excess Nb present, it is accompanied by a changing unit cell size allowing the interpretation that the excess goes on the "B" sites of the unit cell. In this interpretation the excess Nb can be regarded as impurity or source of chemical disorder on the

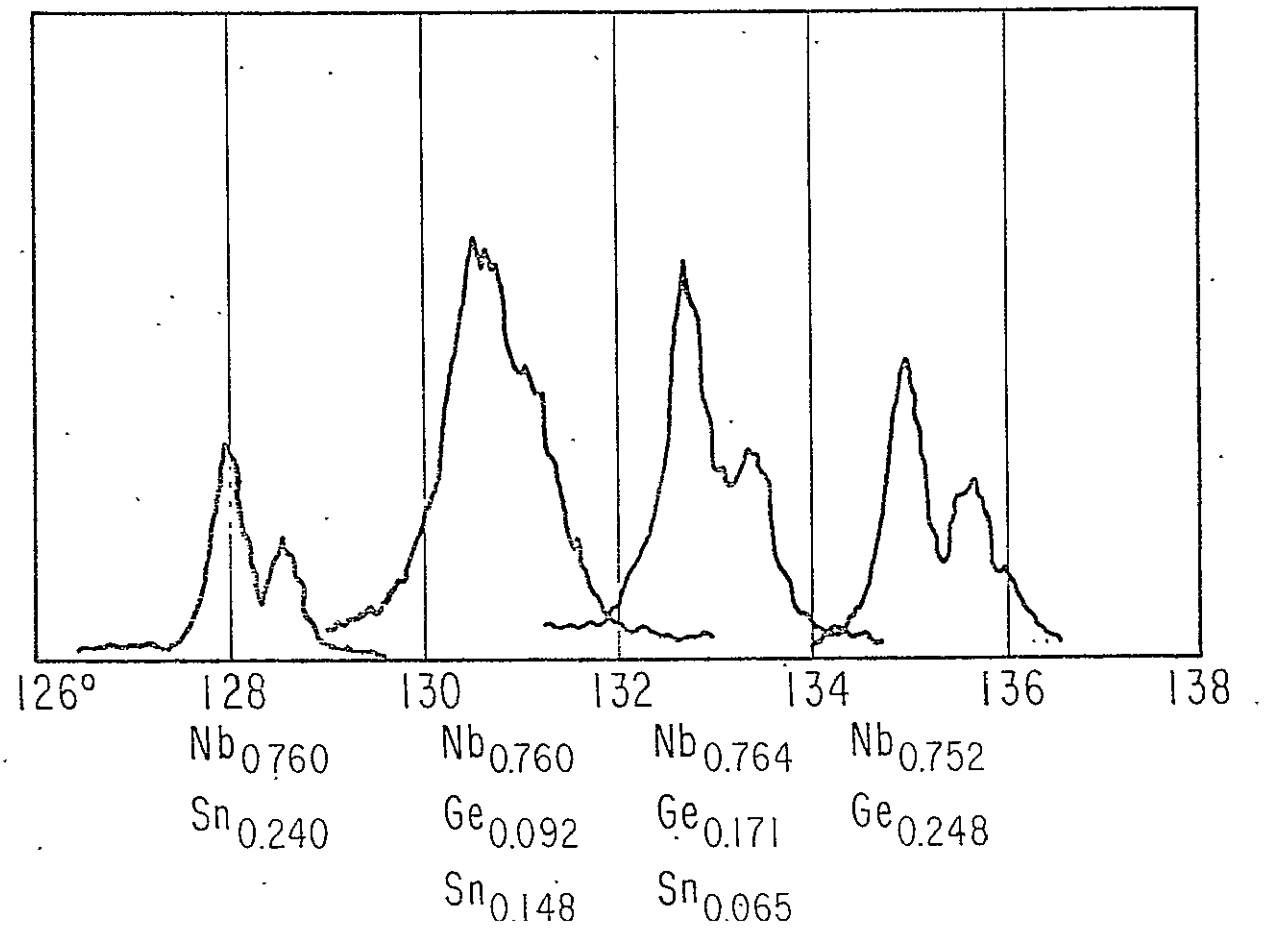

Fig. 7. A-15 {611} x-ray diffraction lines for representative samples in the Nb-Ge-Sn ternary system plotted versus 2θ (x-ray diffraction angle).

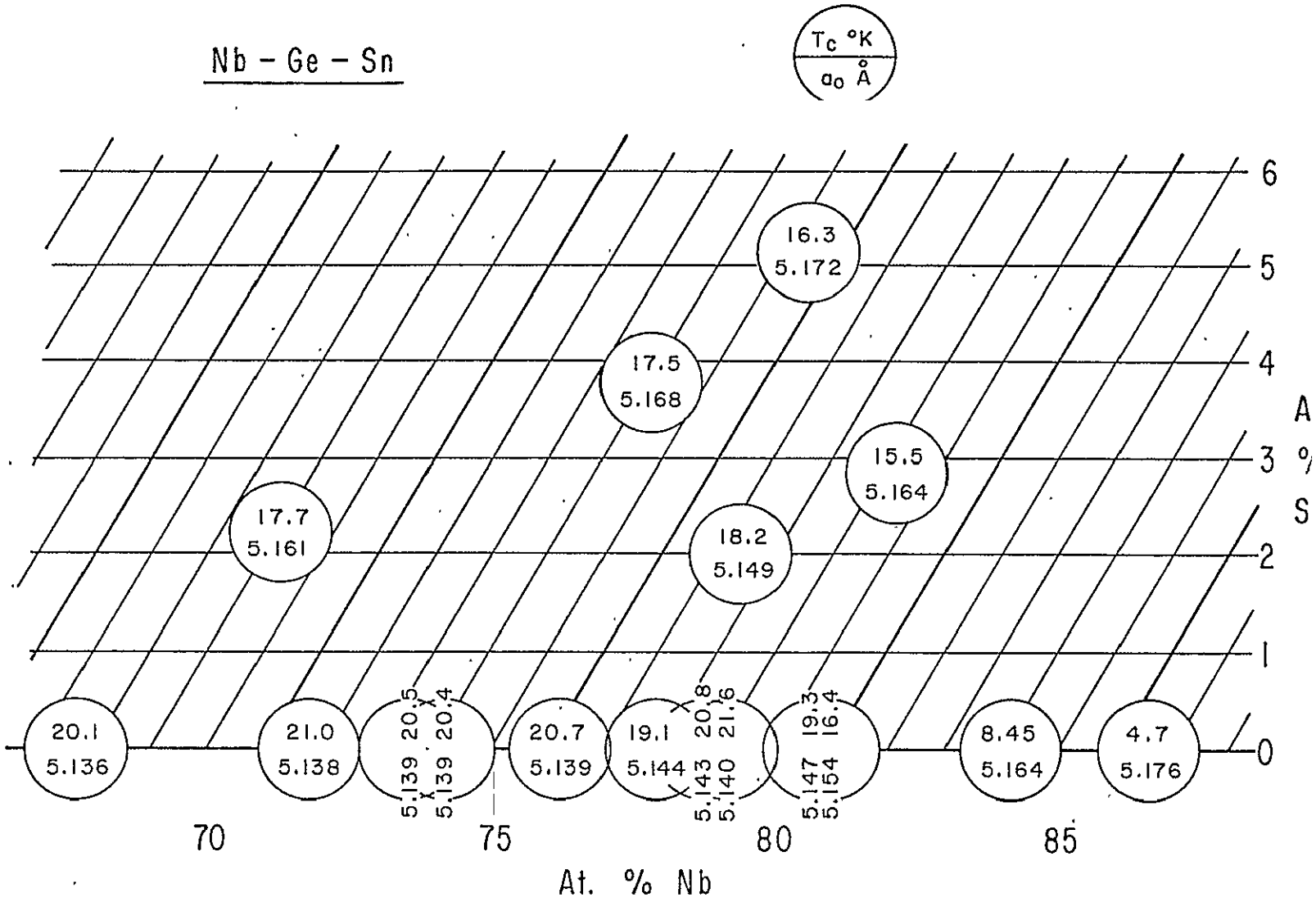
Nb - Ge - Sn
Tc °K
ao Å
16.3
5.172
17.5
5.168
15.5
5.164
17.7
5.161
18.2
5.149
20.1
5.136
21.0
5.138
20.5
20.4
5.139
5.139
20.7
5.139
19.1
20.8
21.6
5.144
5.143
5.140
19.3
16.4
5.147
5.154
8.45
5.164
4.7
5.176
6
5
4
3
2
1
0
At. % Nb
70
75
80
85

Fig. 8

B site. The effect of the resultant disorder is qualitatively similar to the effect of site exchange disorder introduced by irradiation with high energy neutrons for example. Disorder from a variety of sources has been shown to depress T_c and to simultaneously depress the resistance ratio of high T_c A-15 structure materials.[20]

If our chemical analysis results in Fig. 6 were in error in such a way that the compositions near $x \sim 0.5$ contained more than 76 at. % Nb then this would explain the minimum in T_c and Γ. However, we have seen no indication of such a systematic error in the analysis. Another possibility would be that a Nb deficient second phase was co-deposited with the A-15 phase causing it to deviate strongly from 76 at. % Nb, but the diffraction analysis does not support such a possibility. The A-15 lattice parameter data of Fig. 6c) give no suggestion of strong systematic shifts in the Nb concentration. The most straightforward explanation for these data is that T_c and Γ are depressed by the disorder introduced by having both Ge and Sn on the B sites. In this interpretation the effect of disorder present in mixed B atom systems is qualitatively the same as the disorder introduced by Nb deviations from stoichiometry. It is clear that other effects (valence, etc.) in mixed B atom systems could wash out a T_c minimum but in this system the effect of disorder would appear to dominate.

That the diffraction lines show broadening for ternary compositions near $x \sim 0.5$ suggests that there could be additional complexities present in this system due in part to the nonequilibrium nature of the samples. Even A-15 structure pseudobinary systems prepared under conditions nearer to equilibrium show surprising features. Of possible relevance is the fact that a number of them exhibit miscibility gaps.[21, 22] For example, Roeschel and Raub[21] find a deep minimum in T_c in the V_3Si-V_3Ga systems which would be even deeper but for the development of a miscibility gap with two A-15 structures in the middle of the system. To decide if the line broadening is due to similar features in the present nonequilibrium system requires further, more microscopic measurements.

B. NbGeGa System

In order to incorporate even small amounts of Ga into the deposits it was necessary to add large amounts of Ga to the starting ingot, typical ingot compositions being in the vicinity of Nb_3GeGa_2. This observation is in agreement with earlier CVD studies on binary NbGa alloys by Vieland and Wicklund.[23] These authors suggest that Ga is present in the gas phase as a subchloride which deposits by disproportionation to metal and higher metal chlorides. [Preliminary results indicate that reducing the deposition temperature to as low as 700°C enhances Ga deposition as expected for such a reaction.]

Figure 9 shows A-15 lattice parameter and T_c data from ternary samples containing small amounts of Ga deposited at 900°C using our standard flow rates. It can be seen that the addition of Ga to Nb-Ge alters T_c and a_o very little for a wide range of Nb/Ge ratios. At constant Nb content the effect of substituting Ga for Ge is a very slight increase in a_o and a very slight decrease in T_c. There are no strong changes in the phase composition (due to the addition of Ga), over the NbGe binary films as observed in the x-ray diffraction patterns of the films on their alumina substrates. In general the Ga substitutions do not appear to alter strongly the relative amounts of A-15 and "σ" phases. Although T_c is not much affected by Ga substitutions in dilute amounts there are indications that it provides modest increases in J_c and H_{c2} of the NbGe film as they were prepared here.

C. NbGeSi System

Similar to Ga the Si deposition efficiency was low. Consequently large relative amounts of Si were added to the ingot. Typical ingot compositions were in the range $Nb_3GeSi_{0.7}$. Figure 10 shows A-15 lattice parameter and T_c results. These films were prepared at 900°C using the standard flows. The substitution of Si for Ge results in a depression of T_c and, for small amounts of Si, a slight decrease in A-15 lattice parameter. At the same time, however, extra phases appeared in the diffraction patterns from below

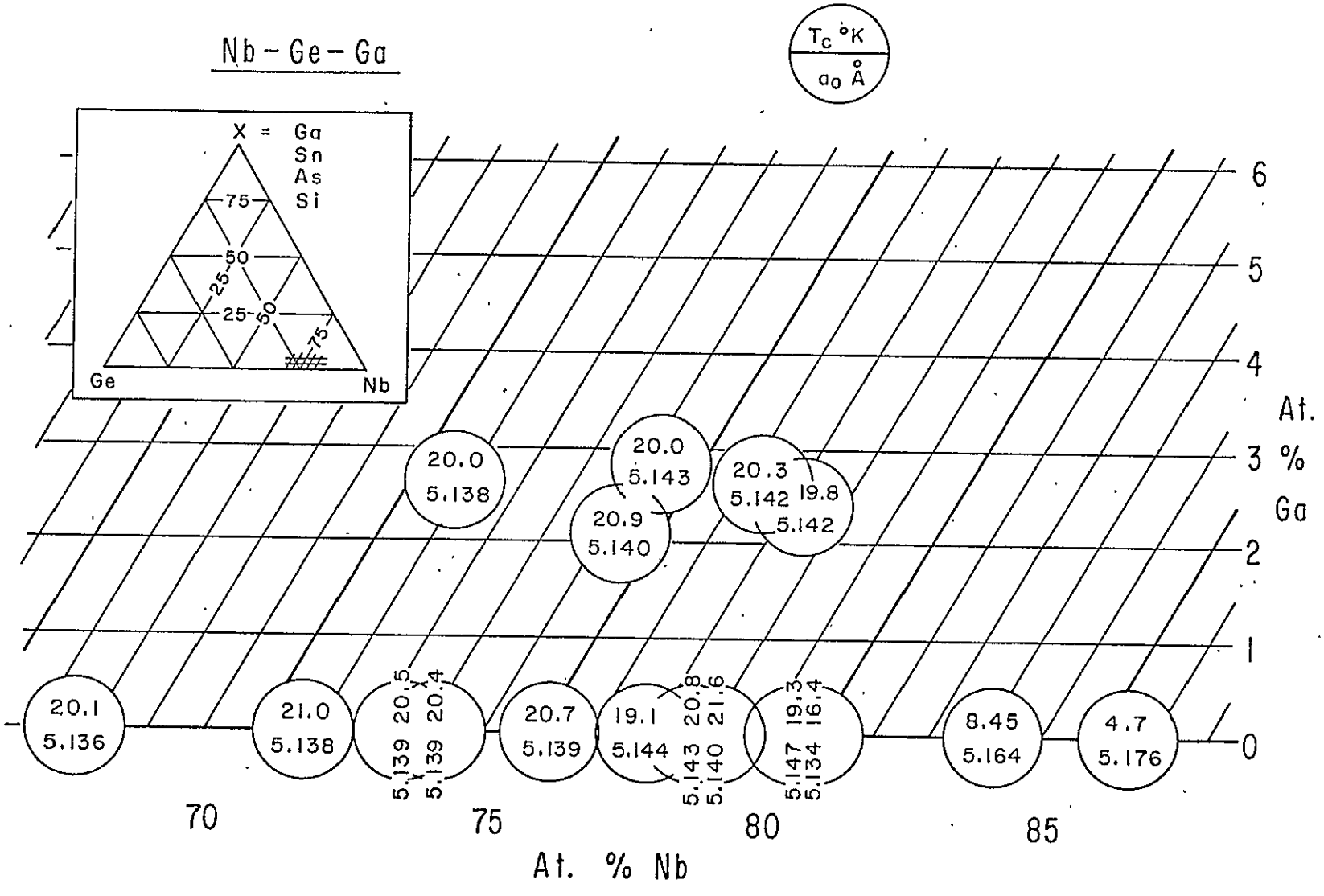
Nb - Ge - Ga
T_c °K
a_o Å
X = Ga
Sn
As
Si
75
50
25-50
25-50
75
Ge
Nb
20.0
5.138
20.0
5.143
20.3
5.142
19.8
5.142
20.9
5.140
20.1
5.136
21.0
5.138
20.5
20.4
5.139
5.139
20.7
5.139
19.1
5.144
20.8
21.6
5.143
5.140
19.3
16.4
5.147
5.134
8.45
5.164
4.7
5.176
6
5
4
3
2
1
0
At. % Ga
70
75
80
85
At. % Nb

Fig. 9

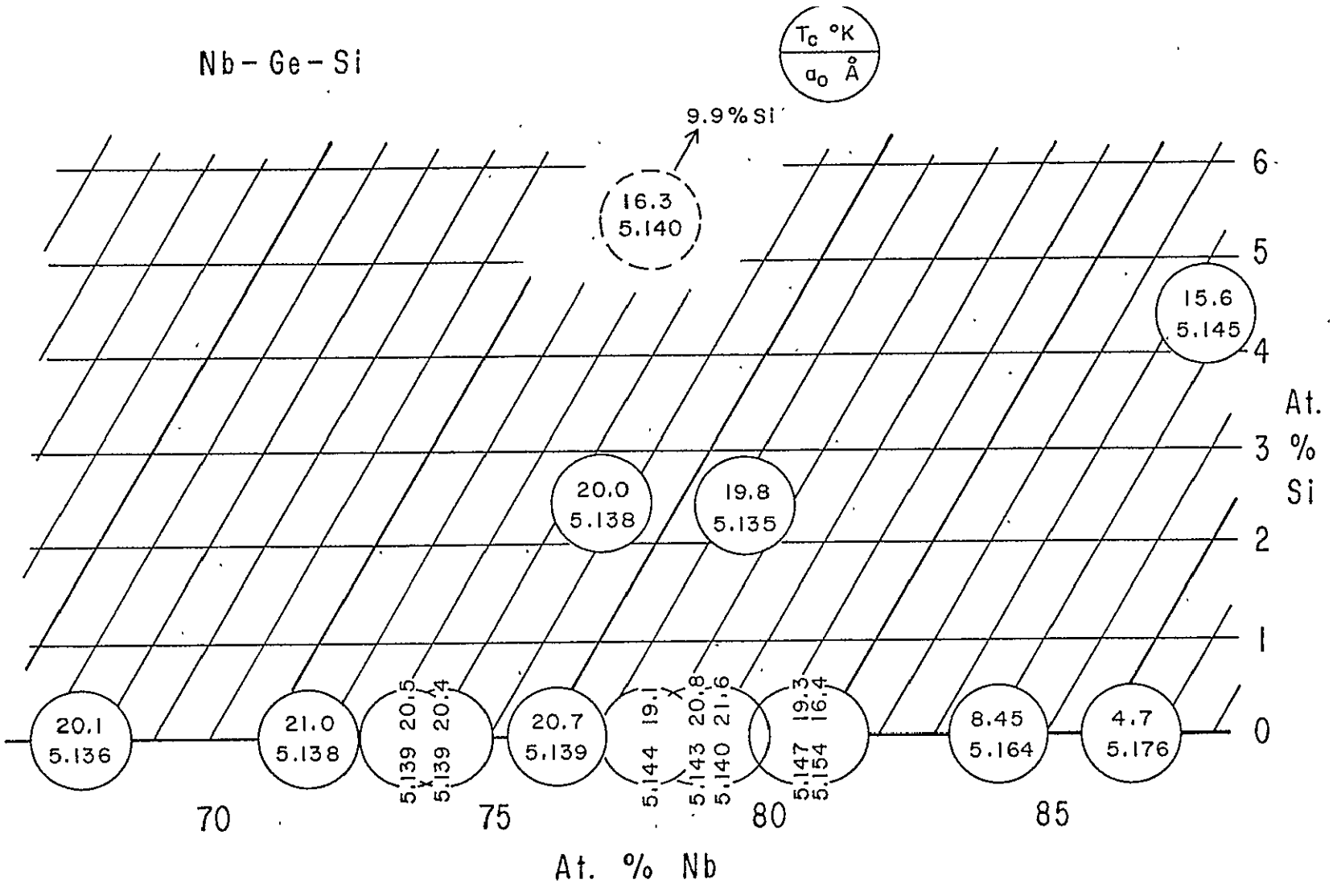
Nb - Ge - Si
T_c °K
a_o Å
9.9% Si
16.3
5.140
15.6
5.145
20.0
5.138
19.8
5.135
20.1
5.136
21.0
5.138
20.5 20.4
5.139 5.139
20.7
5.139
19.1 20.8
5.144 5.143
21.6
5.140
19.3 16.4
5.147 5.154
8.45
5.164
4.7
5.176
0
1
2
3
4
5
6
At. % Si
70
75
80
85
At. % Nb

Fig. 10

the level of detectability without Si to tens of percent with the addition of even small amounts of Si even with Nb contents greater than 75 at. %. Also the diffraction lines of the A-15 phases became quite broad washing out the $\alpha_1 \alpha_2$ doublet separation.

D. NbGeAs System

The effect on the A-15 lattice parameter and T_c at different measured deposit compositions is shown in Fig. 11 . The As was added to the starting ingots, in small amounts, for example, $Nb_3GeAs_{0.05}$. These films were deposited at 900°C using the standard flows. It is found that replacing small amounts of Ge by As increases the A-15 lattice parameter slightly and lowers T_c . In general the x-ray diffraction patterns show broadening of the A-15 diffraction lines, without, however, a strong development of "σ" phase. Since the metallic radius of As is slightly smaller than Ge it is expected that the A-15 lattice parameter would decrease with As substitutions. This is not observed. The most probable explanation is that the addition of As causes the A-15 phase to become more Nb rich by precipitating Nb deficient phases which are below the level of detectability by x-ray diffraction. There was not time to investigate this point in greater detail.

E. Summary of Ternary Results

It is interesting to compare the effect of Sn, Ga, Si and As substitutions, at fixed Nb concentrations, on the A-15 lattice parameter and T_c . Figure 12 shows such data at the concentration of 76 at. % Nb. At this Nb concentration the specimens appear nearly single phase for small amounts of substitution. Clearly all these substitutions decrease T_c , although in the case of Ga the rate is slight. The effect of alloy additions on a_o is of both signs as expected for their metallic radii, except in the case of As as discussed above.

On the basis of these data, we see no evidence of enhanced T_c in Nb_3Ge through alloying these elements for Ge.

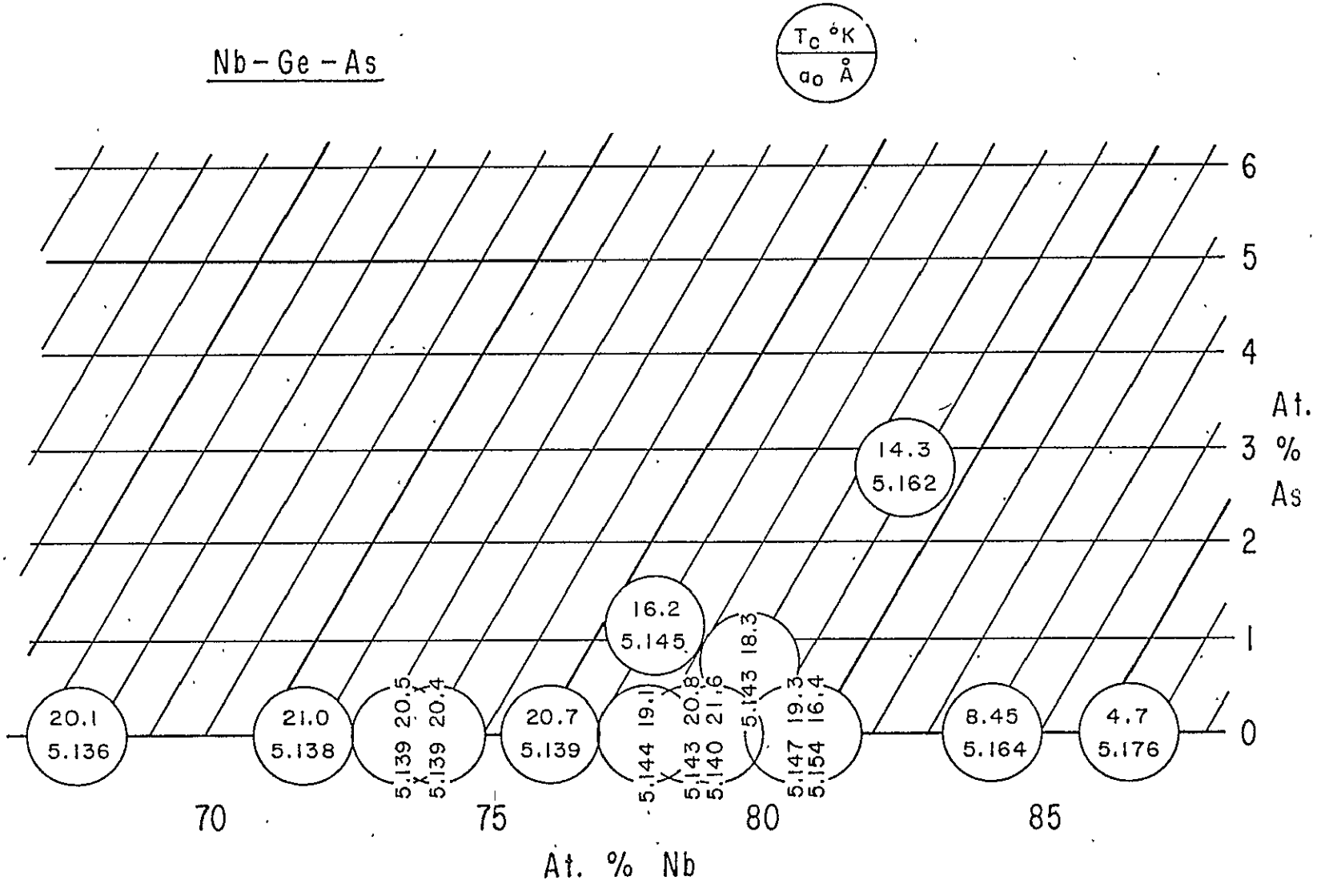
Nb - Ge - As
Tc °K
a₀ Å
6
5
4
3
2
1
0
At. % As
14.3
5.162
16.2
5.145
20.1
5.136
21.0
5.138
20.5
20.4
5.139
5.139
20.7
5.139
19.1
20.8
21.6
5.144
5.143
5.140
18.3
5.143
19.3
16.4
5.147
5.154
8.45
5.164
4.7
5.176
70
75
80
85
At. % Nb

Fig. 11

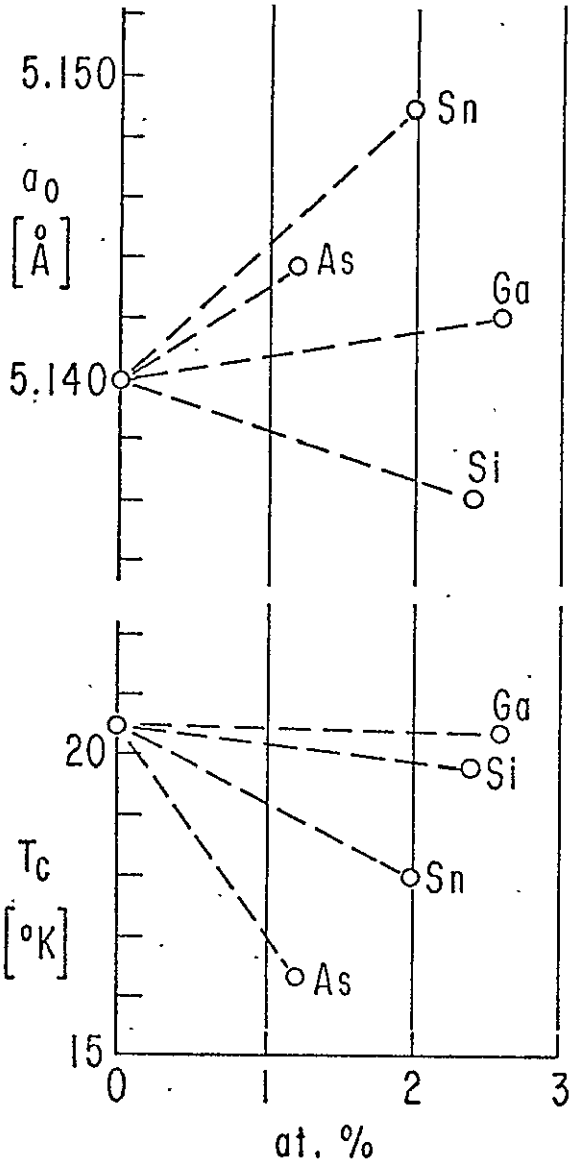

Fig. 12

F. Miscellaneous Other Systems

During the course of this work we found that specimens of Nb_3Al could be quenched from high temperatures, retaining the ductile bcc structure. Crystals of material in this structure were found to be ductile enough to be rolled to one tenth their original thickness. Later short low temperature anneals quickly converted this material to the high T_c ($\simeq$ 18 K) brittle A-15 structure. Details of this work were published last year[24] and are included here as Appendix A.

Some additional investigation was carried out on this material into the kinetics of transformation from the bcc to A-15 structure and into the mechanical properties of the bcc phase. It was found that it could be machined by ordinary techniques used for molybdenum. Some details of this work have been published[25] and are included here as Appendix B.

During the course of this grant we succeeded in growing some single crystals of Nb_3Sn of unusual perfection. The synthesis technique was that of closed tube vapor transport with iodine as the transporting agent. These crystals had resistance ratio from room temperature to T_c of 18. Extrapolating to 0 K suggested a resistance ratio of 50. In any case the material was pure enough to allow observation[26] of DHVA oscillations in magnetic fields above H_{c2}, in the range 20 to 40 T, by colleagues at the high field at the University of Amsterdam. Details of these experiments were published and are included here as Appendix C. The experimental results allow important conclusions to be drawn on the shape of the Fermi surface in Nb_3Sn and thus provide a bench mark for comparison with theory. Some more experimental details and comparison with theory on Nb_2Sn has been published[27] and are included here as Appendix D.

V. Effect of Substrate Materials and Annealing on CVD Films

A. Substrate

To determine the effect of substrate material on the superconducting properties several types of substrates were loaded into the reactor for simultaneous deposition of binary Nb_3Ge. The substrates were accurately placed along side each other at two positions in the reactor. The substrates were alumina, sapphire with the C axis in the plane of the substrate, sapphire with the "R" cut having the C axis about 57° from the substrate, Nb foil of 5 μ thickness, Mo of 25 μ thickness and $LiNbO_3$. The deposition was carried out with standard flows and a deposition temperature of 850°C.

The T_c data obtained from these deposits are shown in Figs. 13 and 14. There is a total spread in T_c in both cases of order 1 K with the deposit on Mo having the lowest value. In order to interpret these T_c data it is useful to compare them with measurements of the thermal expansion of the different substrate materials. Clearly the proper comparison would be between differential thermal contraction between sample and substrate over the range from the deposition temperature, 850°C in this case, and T_c. However, thermal expansion data are not always known in this detail. Accordingly we have taken from the literature[28] the average thermal expansion over the range from room temperature to 900°C unless otherwise noted. These data are shown in the table. Entries 1 to 5 are for the substrate materials found in Figs. 13 and 14. It is clear that Mo is a poor thermal expansion match for Nb_3Ge, putting the superconductor in under tension upon cooling, which corresponds well with the largest depressions of T_c being observed for Mo. The other materials, 1 to 5, have expansion coefficients much closer to that of Nb_3Ge[29] (it should be kept in mind that there is considerable scatter in the literature thermal expansion data).

In other experiments, deposits were prepared on BeO fused quartz and graphite fibers. In these experiments, control deposits were simultaneously prepared on alumina substrates placed along side. As expected

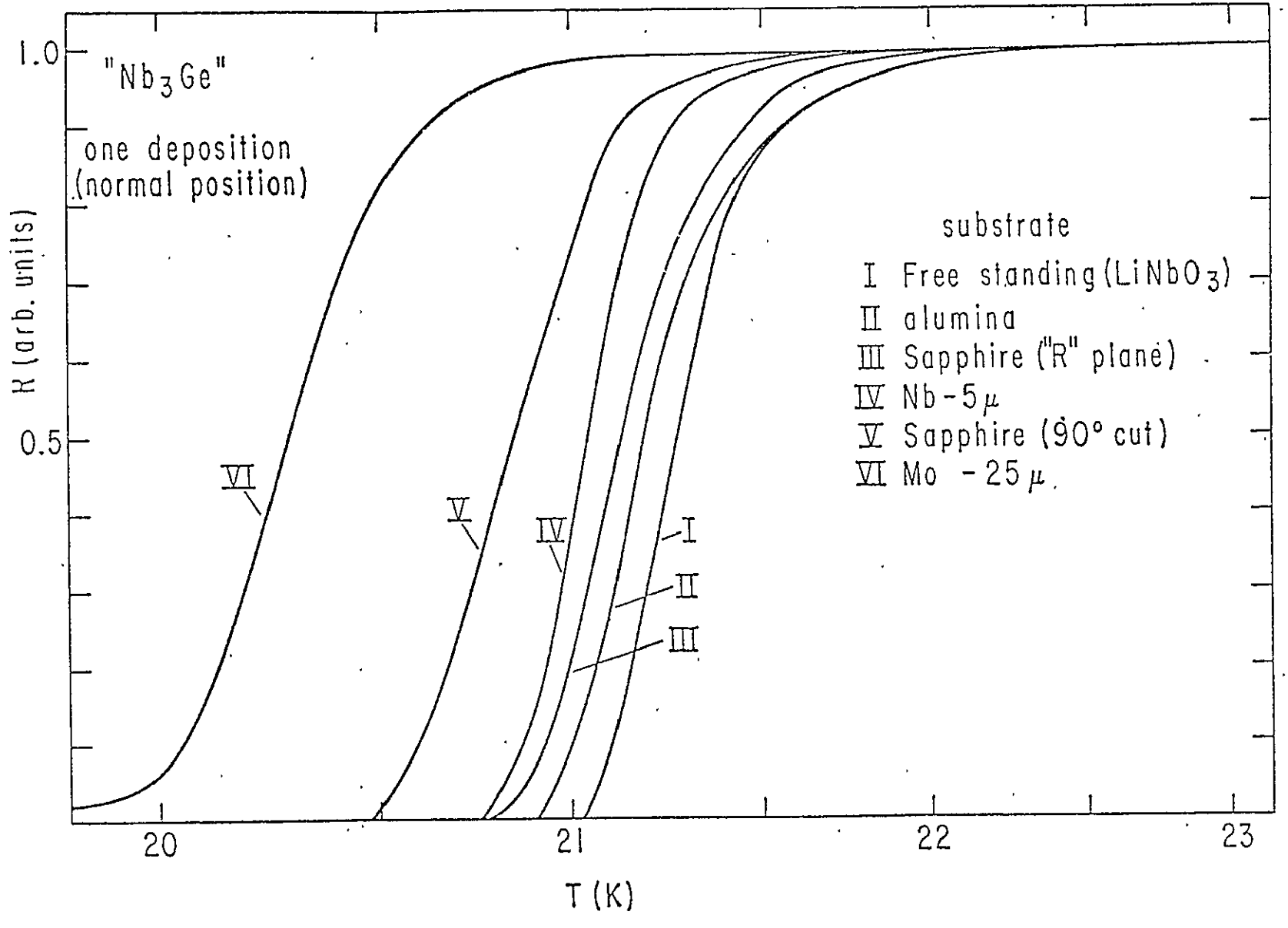
"Nb3Ge"
one deposition
(normal position)
substrate
I Free standing (LiNbO3)
II alumina
III Sapphire ("R" plane)
IV Nb - 5μ
V Sapphire (90° cut)
VI Mo - 25μ
R (arb. units)
1.0
0.5
20
21
22
23
T (K)

Fig. 13

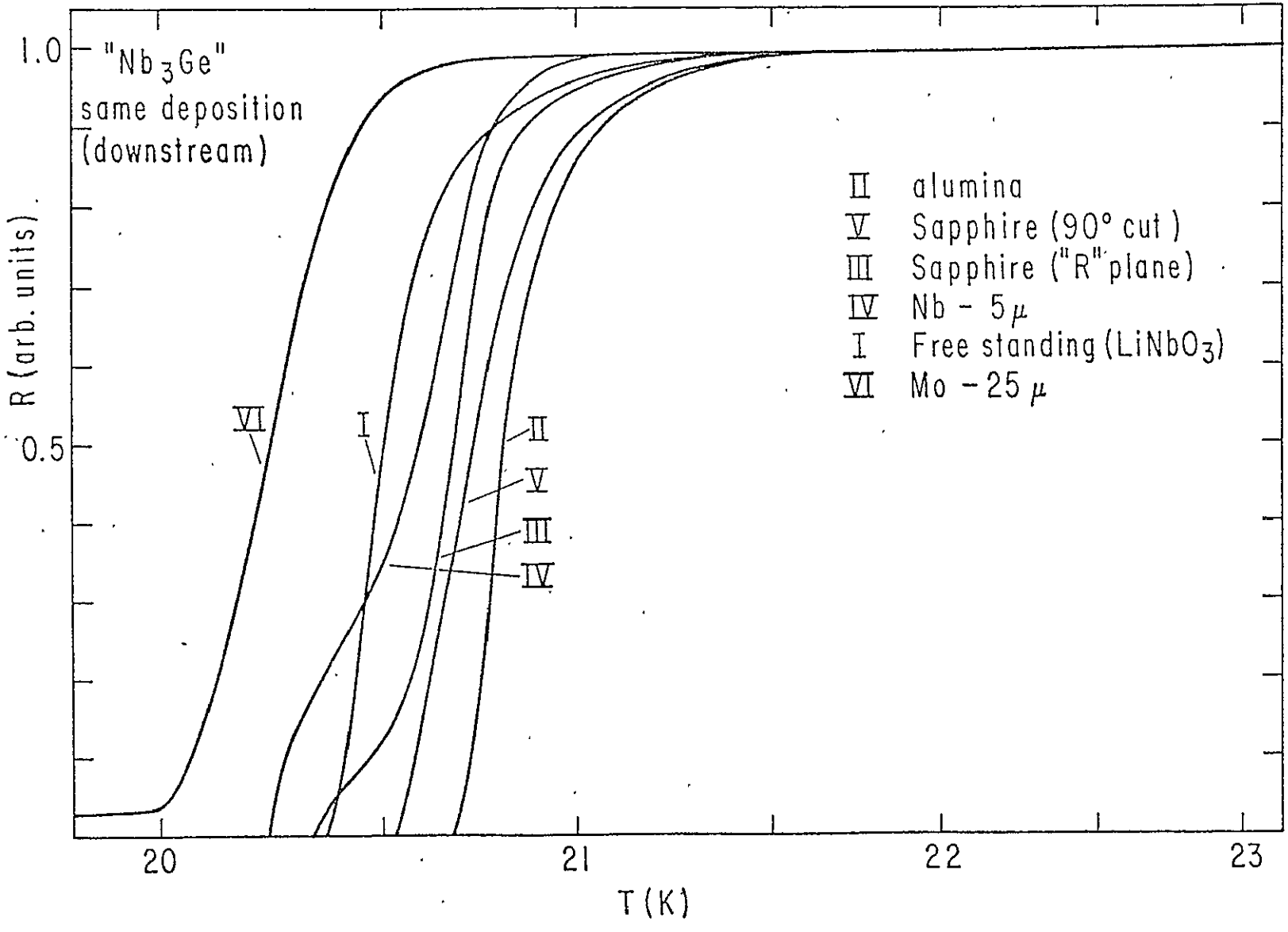
1.0
0.5
R (arb. units)
"Nb3Ge"
same deposition
(downstream)
II alumina
V Sapphire (90° cut)
III Sapphire ("R" plane)
IV Nb - 5μ
I Free standing (LiNbO3)
VI Mo - 25μ
VI
I
II
V
III
IV
20
21
22
23
T (K)

Fig. 14

Table

	Material	Average Thermal Expansion Coefficient (10^{-6})
1)	Nb_3Ge	$\simeq$ 7.7
2)	Alumina (polycrystalline)	8.2
3)	Sapphire	7.8 $\perp$ C 8.6 $\parallel$ C 8.0 = $\overline{\alpha}$
4)	Nb	7.8
5)	Mo	6.5
6)	BeO	8.5
7)	Graphite ("a" axis, $\parallel$ to fiber axis)	1.8

from its favorable thermal expansion coefficients no depression of T_c was observed on BeO (in fact a T_c onset a few tenths of a degree higher than the control was observed although the T_c midpoints were equal). The deposits on quartz and graphite fibers did not prove to be satisfactory. On quartz a large degree of crazing of the deposit and upper layer of substrate was observed. Deposits on the graphite fibers were found to be periodically broken along their lengths. The fibers, furnished by NASA, were of diameter 7 μ with the a axis near the filament direction. The deposit thickness was in the range 5-20 μ. The low thermal expansion along the fiber was evidently enough to open up ~10 μ cracks in the deposit. Consequently, graphite fibers as a substrate material was not pursued further.

In order to investigate the effects of annealing on the deposited material some long term annealing studies were performed. For this study deposits on alumina, 850°C deposition temperature, and free standing deposits, 900°C deposition temperature, which had flaked free from $LiNbO_3$ substrates were used. They were wrapped in Nb foil and placed in carefully outgassed quartz tubing with 150 torr of argon. The annealing was carried at 725° for 3 months. The effect of the annealing on the transition curves can be seen in Fig. 15. The changes in the transitions are slight but T_c seems to be depressed in both cases. No sign of contamination of the deposits or of the foil was found. Annealing material at higher temperatures for times of order hours gave greater depressions of T_c, in agreement with the literature,[30] and as expected from the metastable nature of the high T_c, "stoichiometric" material.

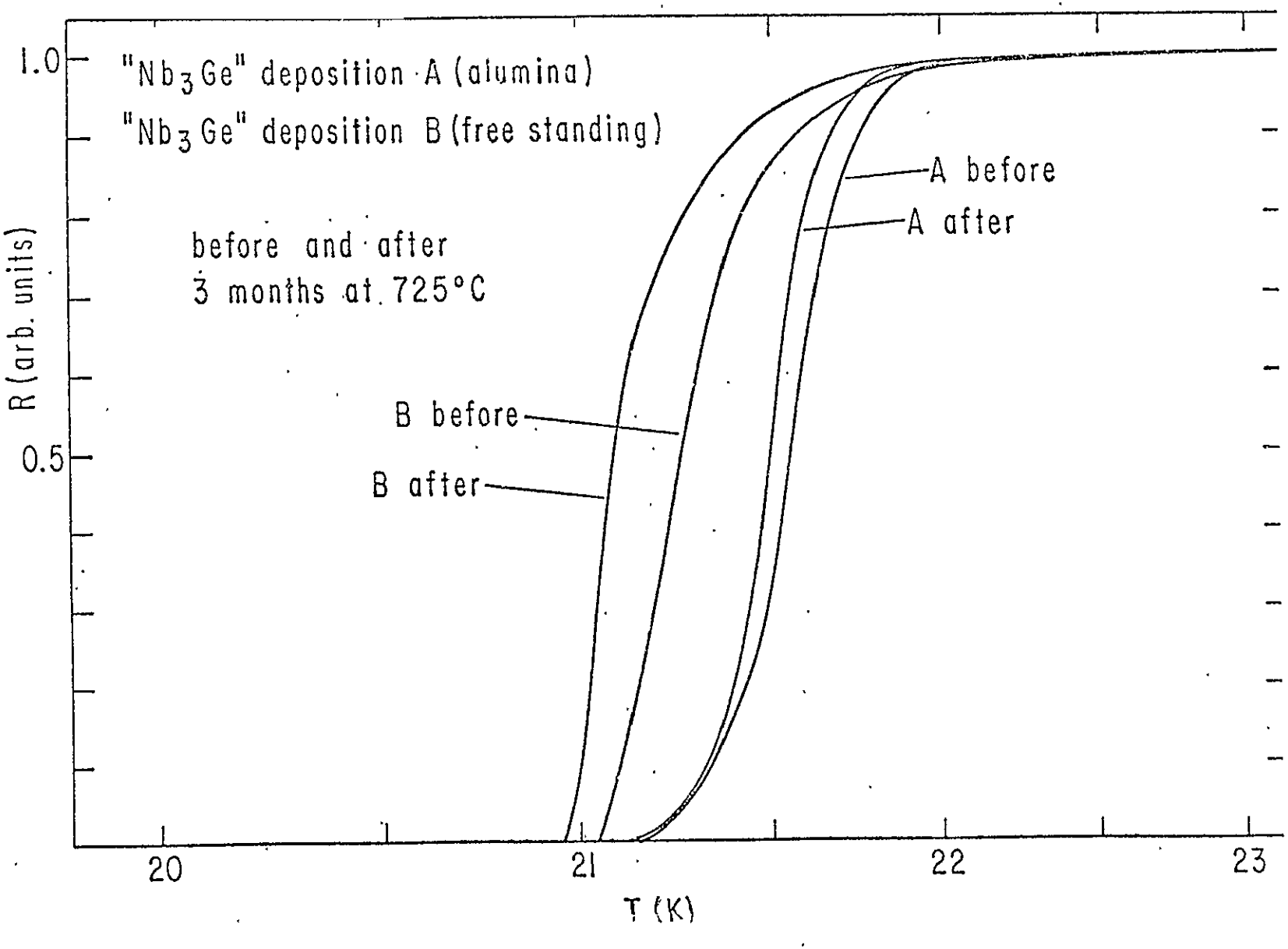
"Nb3Ge" deposition A (alumina)
"Nb3Ge" deposition B (free standing)
before and after
3 months at 725°C
A before
A after
B before
B after
1.0
0.5
R (arb. units)
20
21
22
23
T (K)

Fig. 15

VI. Critical Fields and Current Densities *

Critical Currents in Nb_3Ge Based Pseudobinaries+

Samuel A. Alterovitz*,++ John A. Woollam* John J. Engelhardt** and George W. Webb**

ABSTRACT

We have prepared Nb_3Ge, $Nb_3Ge_{1-x}Ga_x$ and $Nb_3Ge_{1-x}Sn_x$ on heated alumina substrates using CVD. Midresistive transitions were up to 21K and transition widths were as low as 0.3K. Critical currents were measured to 22 Tesla at temperatures from 4.2K to 19K. Effective upper critical fields B^*_{c2} were measured by extrapolating $J_c^{1/2}$ vs B data. Preliminary data show that for small Ga additions, B^*_{c2} increased above the value at x=0. Flux pinning forces vs reduced field $b=B/B^*_{c2}$ do not obey scaling laws, which we explain as being due to inhomogeneous material having a distribution of T_c and B_{c2} values.

I. INTRODUCTION

Among the most promising high critical current superconductors for high field applications are the A-15 structure materials. Critical currents J_c in these materials, and especially[1-4] in Nb_3Ge and Nb_3Sn, have been previously studied in high magnetic fields B. Two flux pinning mechanisms have been found. In CVD grown Nb_3Ge, with high critical currents the main pinning mechanism is σ phase precipitates. In sputtered[2-4] Nb_3Ge, Nb_3Sn, and in clean[4] CVD Nb_3Ge most pinning is at grain boundaries. However, the exact functional forms of the pinning force vs B data for these two mechanisms in (non-epitaxially grown) Nb_3Ge have not been determined due to a lack of scaling of flux pinning forces. This lack of scaling has been postulated to be due to sample inhomogeneity.[6] Very recently[7] homogeneous epitaxial CVD grown Nb_3Ge has been shown to obey the scaling law form proposed by Kramer.[8]

In addition to the interest in binary compounds such as Nb_3Sn and Sn_3Ge, pseudobinaries such as $Nb_3Ge_{1-x}Sn_x$ are expected to have promisingly high values of J_c and B_{c2}. It has been shown experimentally[9,10] that small additions of a third element to a binary A-15 compound (usually Nb_3Sn), can increase the effective upper critical field and the high field critical current. This trend is expected to reverse as the amount of third element added to the binary increases or becomes dominant. In the present paper we report on a study of critical currents in high magnetic fields, and critical fields and temperatures as a function of composition.

II. EXPERIMENTAL METHODS

All samples were prepared by CVD on alumina substrates at 900 C, as described in detail elsewhere.[11] Thicknesses used for calculations were averages from measurements at five sample positions, using SEM, and ranged from 3 to 10μm between samples. Chemical analysis using an electron microprobe determined composition to within one percent. Midresistive point superconducting transition temperatures T_c were determined at UCSD and at NASA and agree with each other to within better than 0.1K. Critical currents were defined by a 100μV/m criterion, unless noise levels forced us to use 500μV/m. In all measurements samples were immersed either in liquid hydrogen or helium, and the temperature was changed by pumping. External fields were supplied by either a 14Tesla superconducting solenoid or by 18.5Tesla or 22.5Tesla Bitter Magnets. The film plane was always perpendicular to the field direction. Resistive transitions were measured by changing the temperature and using a sampling current of 1 mA or less.

III. RESULTS

Critical current densities J_c were measured in twelve samples: Three in the $Nb_3Ge_{1-x}Ga_x$ series and nine in the $Nb_3Ge_{1-x}Sn_x$ series.

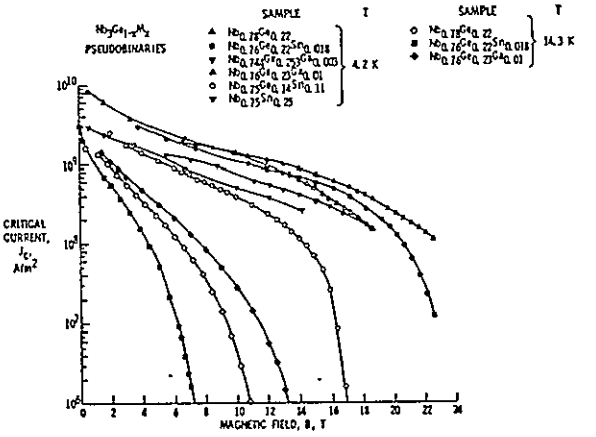

Fig.1. Critical current density J_c vs external magnetic field B, for several pseudobinaries at 4.2K and 14.3K.

For all, J_c was measured at 4.2K, but only six were measured in liquid hydrogen. Representative results for J_c vs B are shown in Fig.1 for two temperatures: 4.2K and

Manuscript received September 28, 1978

+ Part of this work was performed at the Francis Bitter National Magnet Laboratory which is supported by the National Science Foundation

* NASA Lewis Research Center, Cleveland, Ohio 44135

++NRC Senior Research Associate

**Institute for Pure and Applied Physical Sciences, UCSD, La Jolla, California 92093, Research supported by NASA Grant NsG-3055

*Published in IEEE Transactions on Magnetics, MAG 15, 512 (1979).

14.3K. At 4.2K, the external field was not high enough to completely quench superconductivity in some cases. Therefore a simple extrapolation[12-17] to $I_c^{1/2}=0$ was made, where I_c is the experimental critical current. The critical field thus obtained is called the effective upper critical field B^*_{c2}, and is the highest field where currents below the critical current can be carried. Typical extrapolations of $I_c^{1/2}$ vs B are shown in Fig.2. Data are shown for two temperature groups: 4.2K, and in the liquid hydrogen range. A very important feature in this graph is the shape of the $I_c^{1/2}$ vs B plots. For a clean and homogeneous sample $Nb_{0.75}Sn_{0.25}$ (with residual resistivity of $8\mu\Omega cm$) $I_c^{1/2}$ vs B is a straight line. For other samples the plots have positive curvature for temperatures in the liquid hydrogen range, and negative curvatures at 4.2K. The presence of curvature is an important source of error in estimating B^*_{c2}.

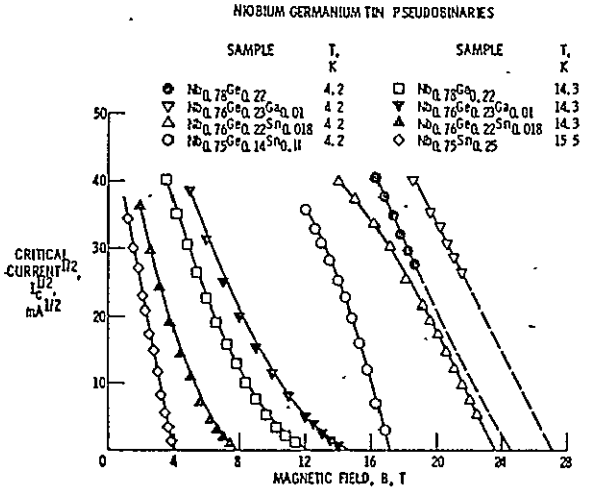

Fig.2. Extrapolations of $I_c^{1/2}$ where I_c is the critical current, vs. the external magnetic field. The value of B at I=0 is the effective upper critical field B^*_{c2}.

For positive curvatures, long extrapolations can yield B^*_{c2} values too low, and negative curvatures can give values too high. Since J_c was measured at 4.2K to 22.5 Tesla in only three samples, and most of the other measurements were made to only 16.5 Tesla, derived B^*_{c2} values could be in error by one to two Tesla. Figure 3 shows B^*_{c2} as a function of third element concentration in Nb_3Ge. There is no simple correlation between the Nb concentration (which varies in the range 74-78 atomic percent) and B^*_{c2}. The dashed portion of the B^*_{c2} curve near a pure Nb_3Sn composition was drawn using values in the literature[7] for B^*_{c2} for materials with similar compositions. Also in Fig.3, T_c^* vs composition is plotted, where T_c^* is the critical temperature, as defined by the zero resistance point using a high sensitivity voltmeter.

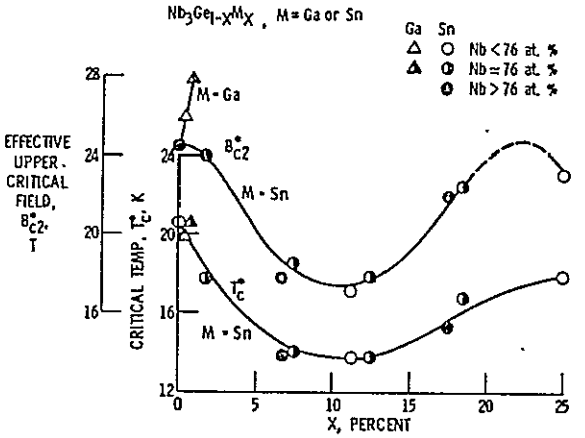

Fig.3. Effective upper critical field B^*_{c2} and effective critical temperature T_c^* vs third element concentration x in $Nb_3Ge_{1-x}M_x$ for all samples.

Selected results for B^*_{c2} in the liquid hydrogen temperature range are shown in Table I, together with midresistive point measurements of B_{c2}.

TABLE I

Upper Critical Fields at Temperatures T≥14.3K

Sample	T, K	B^*_{c2}, T	B_{c2}, T
$Nb_{0.78}Ge_{0.22}$	14.3	11.4	13.7
	16.6	6.93	8.8
	18.6	3.53	4.4
$Nb_{0.76}Ge_{0.22}Sn_{0.018}$	14.3	7.8	9.0
	15.8	4.5	5.65
$Nb_{0.75}Sn_{0.25}$	15.5	4.0	4.1
	16.9	1.57	1.59

Data shown in Table I demonstrate that the clean and homogeneous Nb_3Sn sample has $B^*_{c2}\simeq B_{c2}$, i.e. has a very narrow transition width. The other samples have very wide transitions. Values of B^*_{c2} were obtained by a least squares fit of the four highest field experimental points to a $I_c^{1/2}$ vs B plot. B^*_{c2} depends on the number of points in the fits, and thus introduces uncertainties in B^*_{c2} and thus in b.

The B^*_{c2} values of Table I were used to study scaling of critical currents for temperatures above 14.3K. The pinning force density F was calculated using

$$P = B \cdot J_c \qquad (1)$$

Scaling laws for critical currents are obeyed if[13,16,17]

$$P = c\left[B^*_{c2}(T)\right]^n f(b) \qquad (2)$$

where c and n are constants, $b=B/B_{c2}$ and f(b)

is a function independent of temperature. Usually f(b) is normalized to a maximum value of 1. If P_{MAX} is denoted as the maximum value of the pinning force density at any temperature T, then

$$P_{MAX} = C\left[B_{c2}^{*}(T)\right]^{n} \qquad (3)$$

$$P/P_{MAX} = f(b) \qquad (4)$$

Thus scaling is obeyed if P/P_{MAX} vs b plots for several temperatures are coincident. In Fig.4 three graphs for $Nb_{0.78}Ge_{0.22}$

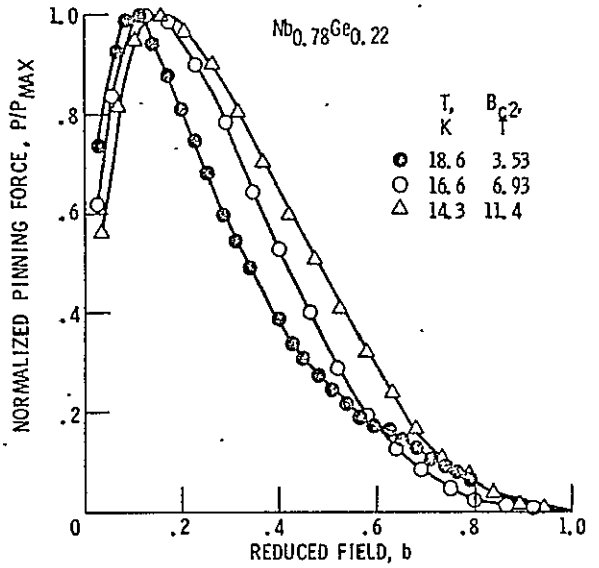

Fig.4.Normalized pinning force P/P_{MAX} vs. reduced field $b=B/B_{c2}$ for $Nb_{0.78}Ge_{0.22}$ for T above 14.5K.

clearly show the absence of scaling. A lack of scaling is unusual[4,16,17] and possible origins are explained in Refs. 15 and 18. In the present case we believe the origin lies in the uncertainty in B_{c2}^{*} values, as determined from I_c^{vs} vs B plots. This influences tests for scaling through determinations of b. Detailed discussions of these effects will be presented elsewhere.

I. DISCUSSION

Preliminary results show that small additions (of the order of one per cent) of Ga added to Nb Ge, can increase the effective upper critical field. This can be explained assuming the dirty limit($\ell \ll \xi_0$) approximation where $B_{c2} \propto \gamma T_c$, where ρ is the resistivity. For example by adding one percent Ga to Nb_3Ge, T_c did not change, while ρ increased from 35 $\mu\Omega$cm to 50 $\mu\Omega$cm. Therefore B_{c2} is expected to rise, although by a smaller factor than the increase in ρ because γ decreases with disorder.[15,18] By increasing the amount of the third element (Sn in our case) both γ and T_c are depressed because of disorder, thus reversing the trend and lowering B_{c2}. A quantitative study of γ as a function of the third element will be published elsewhere.[15]

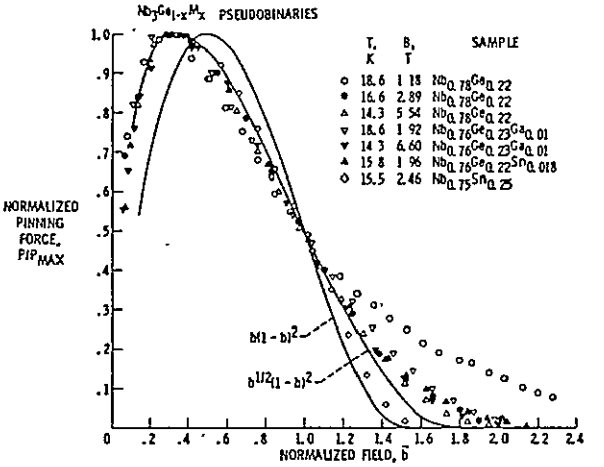

Fig.5.Normalized pinning force vs renormalized field $b=B/\bar{B}$ where $\bar{B} = B(P = 0.5P_{MAX})$ for four samples above 14.5K.

CONCLUSION

From preliminary studies we find that small additions of Ga to Nb_3Ge may enhance the effective upper critical field. We believe that in most (or all) of our samples pinning is at grain boundaries, thus yielding relatively low values of the critical current density. An optimization of J_c can likely be achieved by increasing pinning via σ phase precipitates, or by decreasing grain size, in pseudobinaries containing small amounts of Ga. Scaling over a limited range of b was restored, by circumventing problems in experimentally determining B_{c2}.

Acknowledgement

The authors are grateful to Dr.D.Rubin and Dr.J.Daigle of the Francis Bitter National Magnet Laboratory for their assistance in making high field measurements.

REFERENCES

1. A.I.Braginski, J.R.Gavaler, G.W.Roland, Michael A.Daniel, L.A.Janocko and A.T. Santhanam, IEEE Trans.MAG-13,300(1977).
2. J.R.Gavaler, L.A.Janocko, A.I.Braginski and G.W.Roland,IEEE Trans.MAG-11,192(1977)
3. A.T.Santhanam,J.J.Hafstrom and C.T.Wu, IEEE Trans.MAG-13,315(1977)and private communication.
4. H.Ullmaier,Irreversible Properties of Type II Superconductors, New York, Springer-Verlag Inc.,1975,Ch.5.
5. M.R.Daniel,A.I.Braginski,G.W.Roland,J.R. Gavaler,A.J.Bartlett and L.R.Newkirk, J.Appl.Phys.48,1293(1977).
6. S.A.Alterovitz,J.A.Woollam,John J.Engelhardt and George W.Webb, Phil.Mag. Correspondence, to be published.

7. J.D.Thompson,M.P.Maley and L.R.Newkirk Bull.Am.Phys.Soc.23,322(1978)and J.Appl. Phys.,to be published.

8. E.J.Kramer,J.Electronic Mat.,4,839(1975)

9. D.Dew-Hughes and M.Suenaga, J.Appl.Phys. 49,357(1978).

10. R.Akihama,K.Yasukochi,and T.Ogasawara, IEEE Trans.MAG-13,803(1977).

11. J.J.Engelhardt and G.W.Webb,J.Less Common Metals, to be published.

12. S.A.Alterovitz,J.A.Woollam,L.Kammerdiner, and H.L.Luo,J.Low Temp.Phys.30,797(1978).

13. S.A.Alterovitz and J.A.Woollam, to be published.

14. D.B.Montgomery and W.Sampson,Appl.Phys. Lett.6,108(1965).

15. S.A.Alterovitz,J.A.Woollam,E.J.Haughland, J.J.Engelhardt and G.W.Webb, to be published.

16. E.J.Kramer,J.Appl.Phys.44,1360(1973).

17. S.A.Alterovitz and J.A.Woollam,J.Low Temp Phys.32 (1978).

18. E.J.Kramer,J.Nuclear Mat. (1978).

19. H.Wiesmann,M.Gurvitch,A.K.Ghosh,H.Lutz, O.F.Kammerer and Myron Strongin, Phys. Rev.B17,122(1978)

VII. Conclusions and Recommendations

An unexpected result was the large effect played by "B" site disorder as, for example, in the $Nb_{0.76}(Ge_{1-x}Sn_x)_{0.24}$ set of data where a minimum in T_c is observed. The other ternary alloy systems did not allow as extensive substitutions for Ge as in the Sn, however, in each case there appears to be a T_c depression except for the case of Ga. For Ga there does appear to be a modest increase in J_c and H_{c_2} when dilute amounts of Ga are substituted for Ge. These increases, however, do not exceed values for binary specimens of NbGe prepared by other techniques. Furthermore, the introduction of large amounts of Ga into the CVD process also introduces additional complexities of control having to do with the chemistry of the Ga chlorides. For these reasons, the evidence at this time does not favor the use of Ga substitutions to enhance the superconducting properties of Nb_3Ge prepared by chemical vapor deposition. It does look attractive to study such Ga additions (and others) in Nb_3Ge prepared by sputtering or physical vapor deposition.

The technique of retaining by quenching Nb_3Al in the ductile (low T_c) bcc structure which can be cold worked and then transformed into the high T_c ($\simeq$ 18 K) brittle A-15 structure appears attractive. It has been used to prepare rather complex machined parts with high T_c. The possibility of making some high T_c devices such as SQUIDs seem evident. The more important question of whether or not it can be prepared in quantities large enough for large scale applications in the form of wire or tape remains to be answered. Preliminary measurements of the high field current densities of the material are large enough to warrant further investigation into the factors ultimately limiting the size of specimens which can be prepared in this way. Also worthy of further study is the relationship processing parameters, the grain size of the superconducting material and its critical current density.

VIII. References

1. L. R. Newkirk, F. A. Valencia, A. L. Giorgi, E. G. Szklarz and T. C. Wallace, Proc. 1974 Applied Superconductivity Conference, p. 221; A. I. Braginski and G. W. Roland, Appl. Phys. Letters 25, 762 (1974).
2. J. J. Hanak, Metallurgy of Electronic Materials, G. E. Brook, ed., Interscience, N.Y. (1963), p. 161.
3. J. R. Gavaler, J. W. Miller and B. R. Appleton, Appl. Phys. Letters 28, 237 (1976).
4. R. A. Sigsbee, Appl. Phys. Letters 29, 24 (1976).
5. K. Schulze, J. Fuss, H. Schultz and S. Hofman, Z. Metallkde. 67, 737 (1976).
6. Constitution of Binary Alloys, Second Supplement, Ed. F. A. Shunk, McGraw Hill (N.Y.) 1969, p. 192.
7. Obtained from Kawecki Berylco Industries.
8. G. W. Webb, S. Moehlecke and A. R. Sweedler, Mat. Res. Bull. 12, 657 (1977).
9. B. T. Matthias, T. H. Geballe, S. Geller and E. Corenzwit, Phys. Rev. 95, 1435 (1954).
10. J. H. Carpenter and A. W. Searcy, J. Am. Chem. Soc. 78, 2079 (1956).
11. S. Geller, Acta Cryst. 9, 885 (1956).
12. J. H. Carpenter, J. Phys. Chem. 67, 2141 (1963).
13. B. T. Matthias, T. H. Geballe, R. H. Willens, E. Corenzwit and G. W. Hull, Jr., Phys. Rev. 139A, 1501 (1965).
14. R. Hagner and E. Saur, Proceedings of the 8th International Congress on Low Temperature Physics (LT8), ed. D. R. Davies, Butterworths (London, 1963), p. 358.

15. F. Galasso, B. Bayles and S. Soehle, Nature 198, 984 (1963).

16. N. E. Alekseevskii, N. V. Ageev and V. F. Shamrai, Inorganic Materials, USSR, 2, 1865 (1966).

17. G. Otto, Z. Phys. 215, 323 (1968).

18. J. R. Gavaler, Appl. Phys. Lett. 23, 480 (1973).

19. A. R. Sweedler, D. E. Cox and S. Moehlecke, J. Nuclear Mat. 72, 50 (1978).

20. L. R. Testardi, R. L. Meek, J. M. Poate, W. A. Royer, A. R. Storm and J. H. Wernick, Phys. Rev. B11, 4304 (1975).

21. E. Roeschel and Ch. J. Raub, J. Metall. 26, 29 (1972).

22. F. J. Bachner, J. B. Goodenough and H. C. Gatos, J. Phys. Chem. Sol. 28, 889 (1967).

23. L. J. Vieland and A. W. Wicklund, NASA Final Report for contract NAS3-16060.

24. G. W. Webb, Appl. Phys. Lett. 32, 773 (1978).

25. G. W. Webb, IEEE Trans. Magnetics, MAG-15, 616 (1979).

26. A. J. Arko, D. H. Lowndes, F. A. Muller, L. W. Roeland, J. Wolfrat, A. T. van Kessel, H. W. Myron, F. M. Mueller and G. W. Webb, Phys. Rev. Letters 40, 1590 (1978).

27. A. J. Arko, D. H. Lowndes, A. T. van Kessel, H. W. Myron, F. M. Mueller, F. A. Muller, L. W. Roeland, J. Wolfrat and G. W. Webb, J. de Physique Collogue C6, Vol. 1, C6-1385 (1978) (invited paper to LT15).

28. "Thermophysical Properties of High Temperature Solid Materials," Thermophysical Properties Research Center, Purdue University, Y. S. Touloukian, Ed., Vols, 1 and 4, pt. 1.

29. A. I. Braginski, G. W. Roland, M. R. Daniel, Applied Polymer Symposium, No. 29, 93 (1976).

30. A. R. Sweedler, D. E. Cox, S. Moehlecke, R. H. Jones, L. R. Newkirk and F. A. Valencia, J. Low Temp. Phys. 24, 645 (1976).

IX. Publications of Research Supported in Part or Totally by this Grant

Superconductivity of A-15 Compounds in the System Nb-Ge-Sn Synthesized by Chemical Vapor Deposition, J. J. Engelhardt and G. W. Webb, J. Less Common Metals 62, 89 (1978).

Critical Currents in Nb_3Ge Based Pseudobinaries, S. A. Alterovitz, J. A. Woollam, J. J. Engelhardt and G. W. Webb, IEEE Trans. Magnetics, MAG-15, no. 1, 512 (1979).

Mechanical and Superconducting Properties of Nb_3Al, G. W. Webb, IEEE Trans. Magnetics, MAG-15, 616 (1979).

Cold Working Nb_3Al in the bcc Structure and then Converting to the A-15 Structure, G. W. Webb, Appl. Phys. Lett. 32, 773 (1978).

Fermi Surface and dHvA Effect in the Normal State of High T_c A-15 Superconductors, G. W. Webb, J. de Physique Collogue C6, Vol. 1, C6-1385 (1978) (invited paper to LT 15).

deHaas-van Alphen Effect in the High T_c A-15 Superconductors Nb_3Sn and V_3Si, A. J. Arko, D. H. Lowndes, F. A. Muller, L. W. Roeland, J. Wolfrat, A. T. van Kessel, H. W. Myron, F. M. Mueller and G. W. Webb, Phys. Rev. Letters 40, 1590 (1978).

Comment on 'Influence of Composition on the Superconducting Transition Temperature of Alloys with the A-15 Structure,' G. W. Webb and B. T. Matthias, Solid State Commun. 21, 193 (1977).

The Effect of Composition on T_c in Some High T_c A-15 Structure Superconductors, G. W. Webb, S. Moehlecke and A. R. Sweedler, Mat. Res. Bull. 12, 657 (1977).

Articles Submitted or in Preparation

A Chemical Vapor Deposition Apparatus for the Synthesis of Multicomponent Metallic Compounds, J. J. Engelhardt, submitted to J. Appl. Phys.

Superconductivity of Ternary Alloys Based on High T_c A-15 Structure Nb-Ge, J. J. Engelhardt and G. W. Webb, in preparation.

Critical Currents in A-15 Structure Nb_3Al Converted from Cold Worked bcc Structure, J. A. Woollam, S. A. Alterovitz and G. W. Webb, in preparation.

Cold working Nb_3Al in the bcc structure and then converting to the A-15 structure[a)]

G. W. Webb

Institute for Pure and Applied Physical Sciences, University of California, San Diego, La Jolla, California 92093

(Received 27 December 1977, accepted for publication 23 March 1978)

It is possible to quench gram quantities of stoichiometric Nb_3Al in the ductile body-centered cubic structure which can be cold worked. Later annealing converts this material to the brittle superconducting A-15 structure.

PACS numbers: 74.70.Ps, 74.70 Lp, 81 30.Hd, 81.40.Ef

Superconducting A-15 structure compounds with high transition temperatures are brittle. Their brittleness has slowed but not prevented their development into technological materials.[1] In fact, V_3Ga and Nb_3Sn wires and tapes are now available in a variety of shapes and configurations. Nevertheless, there would be interest in a ductile high-T_c superconducting material. Here we report our initial results on quenching Nb_3Al from high temperatures in the ductile bcc structure which can be cold worked. The quenched and cold-worked-bcc material has a low T_c; it is, however, readily converted to the stoichiometric high-T_c [2,3] A-15 structure (brittle) by annealing. Apparently, this sequence of quenching and cold-working operations has not been done before on Nb_3Al [4] although a similar treatment has been performed on V_3Ga.[5]

Earlier investigations have shown that Nb_3Al can be prepared in the bcc structure by splat quenching from the liquid state[6] and by sputtering onto cooled substrates[6,7] i.e., quenching from the vapor state. The quenched material was transformed to the A-15 structure by annealing. The present method of quenching from under a solidus differs from these in several respects. One is that larger amounts of material are prepared at one time in this case. Another is that the bcc material prepared by quenching from under a solidus consists of large crystals rather than the very-fine-grained polycrystalline product of the other techniques.

Starting ingots are prepared by inverting and melting at least four times in a gettered argon arc furnace. Metallography shows that good mixing occurs on a macroscopic scale. Final compositions are calculated by assuming that the observed weight loss is due to vaporized aluminum; negligible losses during the arc melting of Nb support this assumption. Pieces of an ingot of order 1 g are hung in 0.1-mm Nb wire baskets in a Ta tube furnace of a type described previously.[8] After a high-temperature equilibrating anneal between 1700 and 2000 °C in an argon atmosphere for times of the order of 15 min, the samples are dropped out of the furnace into a Ga-In eutectic liquid quenching bath near room temperature or alternatively onto a copper hearth in which case they cool mainly by radiative heat loss. The Ga-In quench gives an estimated cooling rate in the 10^4 °C/sec range, while the radiative cooling method gives an observed cooling rate of about 10^2 °C/sec. Subsequent annealing is carried out by wrapping the samples in Nb foil and sealing in quartz tubes under 150 Torr of argon; this stage of annealing is terminated by simply removing the tube from the furnace.

The samples used in this investigation are characterized by x-ray diffraction, optical metallography on etched or anodized specimens, microhardness, and transition temperature measurement. Anodization is carried out in concentrated NH_4OH for 5 min at about 30 V.[9] Superconducting transitions are measured resistively at 220 Hz with four indium soldered leads and the temperature is measured with a calibrated Ge resistance thermometer.

After the high-temperature equilibration and quench into GaIn the ingots are found to have their original shape but with several large cracks extending from their interior to their surface. Upon manipulation with tweezers the samples break apart until they appear as

FIG. 1. Photomicrograph of $Nb_{0.74}Al_{0.26}$ annealed at 1925 °C for 20 min then quenched into GaIn near room temperature. The small squares in the grid are 1 mm across. The specimen breaks apart along grain boundaries.

a)Research support by NASA Grant NSG-3055 and by NSF Grant DMR-75-04019.

 0003-6951/78/3211-0773$00.50

a collection of individual crystals, cracking along grain boundaries in which there are impurity phases. Figure 1 shows a photomicrograph of a sample in which individual crystals and collections of a few crystals are evident.

Metallographic examination by etching of a carefully cut unbroken specimen of nominal composition $Nb_{0.74}Al_{0.26}$, quenched from 1925°C into GaIn, reveals about 2 vol% of a second phase located partly in grain boundaries and partly within grains near the sample's center. This second phase is probably A-15 structure material; it anodizes with the same color as the major phase which is bcc by x-ray diffraction. Also, supporting such an identification is its microhardness of 900 kp/mm^2. The major phase has a microhardness of 500 kp/mm^2. A third phase on the 1 vol% level is found in the grain boundaries only. On the basis of its anodization color, it is identified as the Nb_2Al σ phase. The grain boundaries, which comprise only a few volume percent, fracture somewhat upon cutting and polishing, not allowing the observation of other impurity phases such as Al_2O_3.

The isolated individual crystals as seen in Fig. 1 are ductile. For example, a crystal with millimeter characteristic dimensions can be rolled to a sheet 0.1 mm thick without observable cracks. The rolled sheets can be cut (with difficulty) using ordinary wire cutters or slotted with a high-speed alumina cutoff wheel. They cannot be crushed in an ordinary mortar and pestle for x-ray powder diffraction.

X-ray analysis of a rolled sheet having a nominal composition of $Nb_{0.74}Al_{0.26}$ shows only broad diffraction lines of the bcc structure with a lattice parameter of 3.27 Å and an "amorphouslike" broad bump at low angles. This lattice parameter is considerably smaller than that of pure Nb, 3.30 Å, but in good agreement with earlier work for this composition.[6] A resistive measurement of the superconducting transition temperature of a rolled sheet gives a midpoint of 3 K with traces of material superconducting up to 11 K. Other samples similarly treated have about the same midpoint but even less high-temperature traces of superconductivity. These data are to be contrasted with the transition temperature over 18 K for A-15 structure Nb_3Al.[3,6] After a second anneal at lower temperatures, x-ray powder diffraction shows only broad lines of an A-15 major phase, a weak second phase, and no indication of bcc material remaining. Following the second anneal, the transition temperature rises to the neighborhood of 17 K, exact values depending on thermal treatment as shown in Fig. 2. Similarly, the microhardness increases from 500 kp/mm^2 in the bcc structure to 1500 kp/mm^2 in the transformed A-15 structure (approximate value only because of specimen cracking during measurement).

Available data suggest that the rate of conversion of the bcc phase to the A-15 phase is quite high at 950°C. Complete conversion occurs in 40 min; shorter times have not been examined. The data are too few to discuss the conversion rate at 700°C yet. Slowing the quenching rate to 10^2 °C/sec by cooling through radiative heat loss produces specimens which show only lines of the A-15

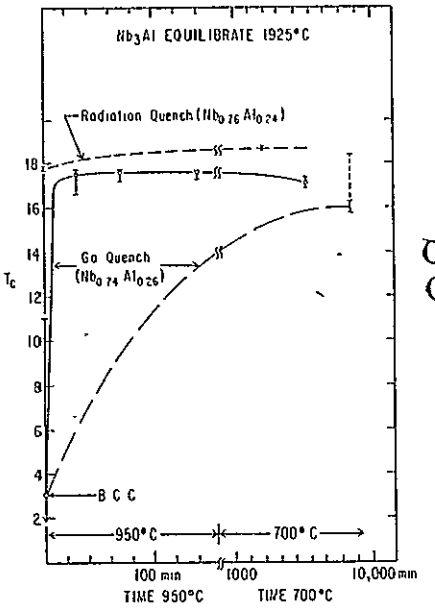

FIG. 2. Transition temperature versus annealing treatment data. The data points are transition midpoints and the error bars show the 10—90% completion points of the resistive transitions. The dotted extension to the datum on the far right indicates a tail to 18.4 K. The dotted curve are guides for the eye only.

phase after quenching and transition temperatures to 18.7 K as shown in Fig. 2.

The present results are not in good agreement with a widely quoted phase diagram[10] for the Nb-Al system. They are, however, in substantial agreement with a less well-known diagram[11,12]; briefly this work describes the A-15 phase as forming by a peritectoid reaction between the bcc α solid solution and the Nb_2Al σ phase.[11,12] At higher temperatures, near 1925°C, the α solid-solution phase boundary extends out to 25 at.%.[12] A recent study[13] of the A-15 phase boundaries is in better agreement with the diagram in Refs. 11 and 12. Where comparison is possible, our own results[14] are in agreement also.

There are a number of points here requiring further investigation. The effect on the superconducting properties of different annealing temperatures and times will have to be investigated. Of particular interest will be measurements of the critical current density in these materials and its response to different annealing treatments.

I am indebted to Z. Fisk for valuable discussions and to A.R. Sweedler for reading the manuscript and calling my attention to Ref. 13.

[1]C.C. Koch and D.S. Easton, Cryogenics 17, 391 (1977).
[2]E.A. Wood, V.B. Compton, B.T. Matthias, and E. Corenzwit, Acta Crystallogr. 11, 604 (1958).
[3]R.H. Willens, T.H. Geballe, A.C. Gossard, J.P. Maita, A. Menth, G.W. Hull, Jr., and R.R. Soden, Solid State Commun. 7, 837 (1969).
[4]N.N. Ganzhula, V.I. Latysheva, V.M. Pan, and K.V. Chuistov, Metallofizika 36, 107 (1971). These authors inves-

tigated two-phase NbAl alloys consisting of an α solid-solution matrix in which is imbedded a precipitate of off-stiochiometric A-15 phase with a T_c of 14 K.
[5]E.M. Savitskii, V.V. Baron, Yu.V. Efimov, M.K. Bychkova, and L.F. Myzenkova, *Superconducting Materials* (Plenum, New York, 1973), p. 392.
[6]L. Kammerdiner and H.L. Luo, J. Appl. Phys. 43, 4728 (1972). This investigation was concerned with NbAl material splat quenched from the liquid state. As quenched the body-centered cubic Nb structure was observed out to $Nb_{0.5}Al_{0.5}$.
[7]R. Wang and S.D. Dahlgren, Metall. Trans. 8A, 1763 (1977).
[8]G.W. Webb and R.E. Miller, Rev. Sci. Instrum 44, 1542 (1973).
[9]A. Müller, Z. Naturforsch. A 25, 1659 (1970).
[10]C.E. Lundin and A.S. Yamamoto, Trans. AIME 236, 860 (1966).
[11]V.N. Svechnikov, V.M. Pan, and V.I. Latysheva, Metallofizika 32, 28 (1970).
[12]V.M. Pan and V.I. Latysheva, Metallofizika 33, 38 (1971).
[13]S. Moelecke, Ph.D. thesis (University of Campinas, Brazil, 1977) (unpublished).
[14]For additional discussion, see G.W. Webb and B.T. Matthias, Solid State Commun. 21, 193 (1977).

MECHANICAL AND SUPERCONDUCTING PROPERTIES OF Nb_3Al

George W. Webb*

ABSTRACT

Nb_3Al can be quenched from under a solidus into the low T_c ductile BCC structure. In the BCC structure a variety of cold working operations can be performed on it without fracture. Later annealing converts this material to the high T_c brittle A-15 structure.

Alloys with the composition Nb_3Al can be quenched from under a solidus into the body centered cubic structure. In this structure they are ductile enough to be rolled to one tenth of their original thickness or machined by ordinary techniques.[1] The body centered cubic material exhibits a low transition temperature (T_c) with transition midpoints near 3 K; however, it is readily converted by annealing to the stoichiometric high T_c A-15 structure with transition midpoints approaching 18 K. Evidently this sequence of quenching, cold working and annealing operations has not been carried out on Nb_3Al [2] before, although a similar treatment was performed on V_3Ga.[3]

Samples of composition near $Nb_{0.75}Al_{0.25}$ are given a high temperature equilibrating anneal[4] between 1700 and 2000°C in an argon atmosphere for times of order 15 minutes[5] and then are dropped out of the furnace into a room temperature Ga-In eutectic liquid quenching bath with an estimated cooling rate of 10^4°C/sec or alternatively onto a copper hearth for a cooling rate of 10^2°C/sec. Later low temperature annealing, carried out by wrapping the samples in Nb foil and sealing in quartz tubes under a 150 torr of argon, is terminated by removing the tube from the furnace

After the initial high temperature equilibration and quench into GaIn the ingots are found to have their original shape but with large cracks extending from their interior to their surface. Upon manipulation with tweezers the samples break apart along grain boundaries, until they appear as a collection of either individual crystals[1] or a few crystals adhering together. Laue back reflection photographs show only well developed spots indicating that many of the individual crystals (grains) are single.

The individual crystals are ductile. They can, for example, be rolled into sheets one tenth their original thickness. X-ray diffraction on rolled sheets show only lines of the BCC structure with lattice parameters appropriate to their composition.[6] A variety of cold working operations can be performed on the BCC material which the brittle A-15 structure would not tolerate without fracturing. For example, it can be rolled, ground, or drilled. Figure 1 shows a part of a quenched ingot containing several crystals of BCC $Nb_{0.75}Al_{0.25}$. They have been first compressed slightly between opposed pistons to form parallel flat surfaces. Although the alloy is tough, it can be drilled through and tapped as shown using standard tools and techniques.[7]

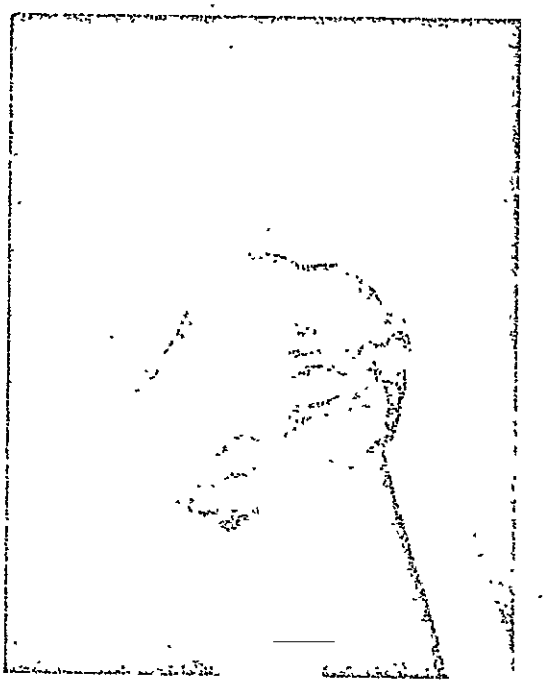

Fig. 1 A BCC specimen of $Nb_{0.75}Al_{0.25}$ quenched from 1925°C. It has been drilled and tapped through with an 0-80 tap. The specimen is supported by an ordinary 0-80 machine screw which is held in tweezers. The hole is too close to one side allowing the threads to break through in places.

The T_c of the as quenched BCC phase having composition near Nb_3Al is about 3 K, as shown in Fig. 2. In this sample there are no signs of superconductivity above 3.23 K, indicating the absence of A-15 structure material. Following an anneal at 950°C for only 36 minutes the T_c rises to 17.7 K (midpoint) as shown and the BCC diffraction lines disappear to be replaced by lines of the A-15 structure.

Quenched BCC specimens do, however, sometimes show signs, by superconductivity and/or metallographic examination, of A-15 filaments in the BCC major phase. For example, metallographic examination of a carefully cut unbroken and etched specimen of nominal composition $Nb_{0.74}Al_{0.26}$, quenched from 1925°C into GaIn, reveals about 2 volume percent of a second phase located partly in grain boundaries and

Manuscript received September 28, 1978.

*Institute for Pure and Applied Physical Sciences, University of California, San Diego, La Jolla, CA 92093.

0018-9161/79/0100-0616$00.75 © 1979 IEEE

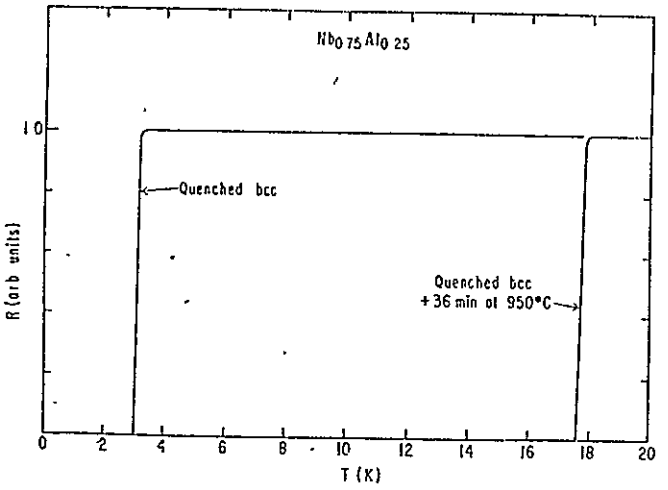

Fig. 2. The resistance versus temperature of $Nb_{0.75}Al_{0.25}$ annealed at 1925°C and quenched into GaIn. The data were measured by the usual 4 probe technique at 220 Hz on a crystal which had been reduced by 90% by rolling into a 4 mil sheet, surface ground and sliced with an abrasive wheel. Note how the low temperature anneal raises T_c from 3 K to 18 K.

partly within grains near the sample center. This second phase is probably A-15 structure material; it anodizes[8] with the same color as the major phase which is body centered cubic by x-ray diffraction. Also supporting such an identification is its microhardness of 900 kg/mm^2. The major phase has a microhardness of 500 kg/mm^2. A third phase on the one volume percent level is found in the grain boundaries only. On the basis of its anodization color, it is identified as Nb_2Al σ phase. A resistive measurement of the superconducting transition in a rolled sheet of this sample displays a midpoint of 3 K with, however, traces of material superconducting to above 11 K as shown by the BCC point in Fig. 3. X-ray analysis of this sheet shows only broad diffraction lines of the body centered cubic structure with a lattice parameter of 3.27 Å, as expected,[6] and a low intensity broad bump at low angles. An unrolled piece of the same sample shows a broad higher resistive transition with a midpoint of 13 K and traces of superconductivity almost to 16 K. It is our assumption that the higher T_c is due to filaments of the above mentioned A-15 material within grain boundaries and in the interior of grains and further that the rolling operation depresses the overall transition by damaging these filaments. After short second anneals at 950°C (or longer ones at 700°C) on quenched and rolled material, x-ray powder diffraction shows only broad lines of an A-15 major phase, a very weak second phase and no signs of remaining BCC material. Following the second anneal, the transition narrows and rises to the neighborhood of 17 K to 18 K, exact values depending on thermal treatment as shown in Fig. 3. Similarly, the microhardness increases from 500 kg/mm^2 in the BCC structure to about 1500 kg/mm^2 in the transformed A-15 structure (approximate value only because of specimen cracking during measurement).

At 950°C the rate of conversion of the BCC phase to the A-15 phase occurs in less than 36 minutes;

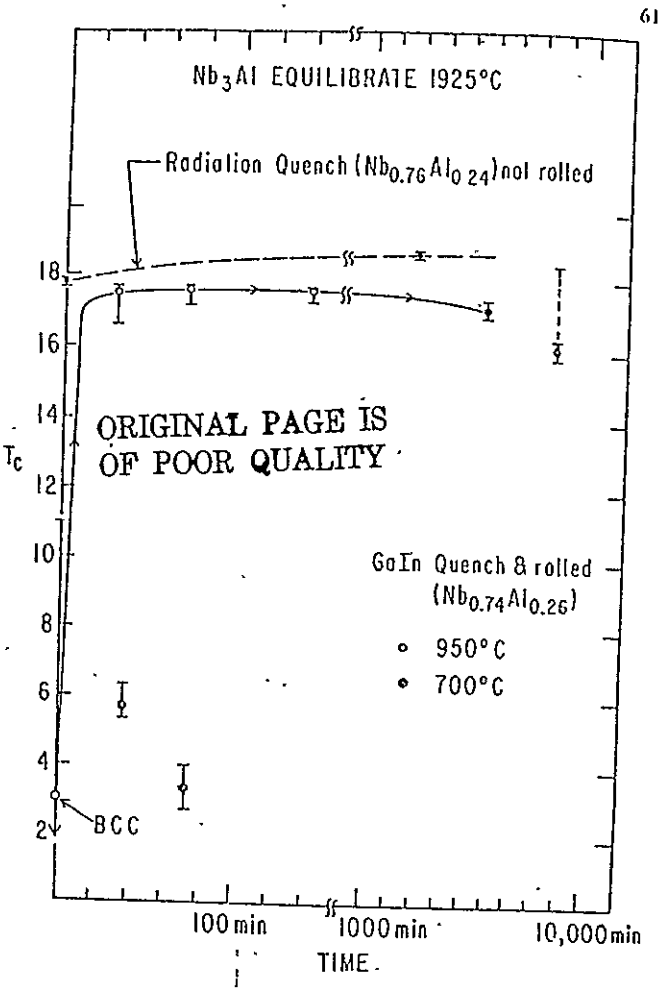

Fig. 3. Resistive transition temperature versus annealing treatment. The data points are transition midpoints and the error bars show where the 10%-90% completion points of the transitions. The three unconnected 700°C points are from three different pieces of a quenched specimen. The dotted extension to the datum on the far right indicates a tail to 18.4 K.

shorter times have not been examined. The few x-ray and T_c data at 700°C show that the rate of conversion is much slower than at 950°C: at 70 minutes the transformation appears to have begun at 70 minutes and to be complete by 6 days. Annealing a BCC specimen of composition $Nb_{0.74}Al_{0.26}$ at 1700°C for 30 minutes and quenching into GaIn shows a complete conversion to a two phase large microstructure consisting of an A-15 phase of lattice parameter 5.184 Å and significant amounts of Nb_2Al σ phase. From the lattice parameter we estimate[8] the composition of the A-15 phase to be about $Nb_{0.76}Al_{0.24}$.

The table shows some T_c data for a specimen of nominal composition $Nb_{0.76}Al_{0.24}$. After quenching into GaIn from 1925°C it is found to be single phase BCC. Annealing at 1700°C for 30 minutes followed by quenching into GaIn converts this material to a single phase having the A-15 structure with a lattice parameter of 5.184 Å. This anneal time is probably sufficient to establish equilibrium for this initial microstructure at this temperature. The material annealed at or below 950°C might be in a nonequilibrium state and is so according to the literature.[9]

TABLE

$Nb_{0.76}Al_{0.24}$	T_c(K) 90%	50%	10%	X-Ray Results
1) 1925°C quenched, not rolled	16.0	15.1	9.0	BCC
2) 1925°C quenched, rolled	3.8	3.3	3.3	BCC
3) 1) + 30 min/1700 quenched	16.1	15.9	15.2	A-15
4) 1) + 3) + 70 min/ 950°C	17.4	17.3	16.9	A-15
5) 2) + 70 min/950°C	17.9	17.8	17.7	A-15

Where comparisons can be made, our results are in substantial agreement with a published phase diagram for Nb-Al.[9, 10] This diagram describes the A-15 phase as forming with the composition 26 at. % Al at 1730°C by a peritectoid reaction between BCC alpha solid solution and the Nb_2Al σ phase. At higher temperatures, near 1925°C, the alpha solid solution phase boundary extends out to 25 atomic percent.[10] Another recent study[11] of the A-15 phase boundaries are also in substantial agreement with the above mentioned diagram except that the peritectoid composition is put closer to 24 at. % Al. The present results support this refinement.

There are several remarks which can be made about the practical significance of fabricating Nb_3Al by the technique described here. It is now fairly well established that this technique is suitable for fabricating rather complex shapes of Nb_3Al having a final T_c of 18 K. The volume of material available for such fabrication is not yet known. Another conclusion is that this technique will be useful for critical current density studies because the grain size of the A-15 phase (and other phases) can be controlled by cold work of the BCC structure and subsequent annealing treatment. To decide if this technique will be a practical means for the production of large quantities of superconducting wire or tape requires more investigation, however the results continue to be promising.

ACKNOWLEDGMENTS

I am indebted to Z. Fisk for valuable discussions and to A. R. Sweedler for valuable discussions and for calling my attention to reference 11. This research has been supported by NSF Grant DMR-77-23774 and NASA Grant NSG-3055.

REFERENCES

1. G. W. Webb, Appl. Phys. Letters, 32, 773 (1978).

2. N. N. Ganzhula, V. I. Latysheva, V. M. Pan and K. V. Chuistov, Metallofizika, Inst. Metallofiz., Kiev, USSR, 36, 107 (1971). These authors investigated two phase NbAl alloys consisting of an alpha solid solution matrix in which is imbedded a precipitate of off stoichiometric A-15 phase with a T_c of 14 K.

3. E. M. Savitskii, V. V. Baron, Yu. V. Efimov, M. K. Bychkova and L. F. Mysenkova, Superconducting Materials, New York: Plenum Press, 1973, p. 392.

4. G. W. Webb and R. E. Miller, Rev. Sci. Instrum., 44, 1542 (1973).

5. Tests show that the weight change due to evaporation corresponds to the loss of ≤ 1 at. % Al out of 25 at. % Al present, if averaged over the whole specimen. The loss is observed to be mainly from the specimen surface.

6. L. Kammerdiner and H. L. Luo, J. Appl. Phys. 43, 4728 (1972).

7. Trichlorethane, recommended for machining molybdenum, was used as a coolant/lubricant. No attempt has been made yet to optimize machining conditions.

8. A. Müller, Z. Naturf., 25a, 1659 (1970).

9. V. N. Svechnikov, V. M. Pan and V. I. Latysheva, Metallofizika, Inst. Metallofiz., Kiev, USSR, 32, 28 (1970).

10. V. M. Pan and V. I. Latysheva, Metallofizika, Inst. Metallofiz., Kiev, USSR, 22, 54 (1968); ibid., 33, 38 (1971).

11. S. Moehlecke, Ph. D. Thesis, University of Campinas, Brazil, 1977.

VOLUME 40, NUMBER 24 PHYSICAL REVIEW LETTERS 12 JUNE 1978

de Haas–van Alphen Effect in the High-T_c $A15$ Superconductors Nb_3Sn and V_3Si

A. J. Arko
Materials Science Division, Argonne National Laboratory, Argonne, Illinois 60139

and

D. H. Lowndes
Department of Physics, University of Oregon, Eugene, Oregon 97103, and Physics Laboratory, University of Nijmegen, Nijmegen, The Netherlands

and

F. A. Muller, L. W. Roeland, and J. Wolfrat
Natuurkundig Laboratorium, University of Amsterdam, Amsterdam, The Netherlands

and

A. T. van Kessel, H. W. Myron, and F. M. Mueller
Physics Laboratory, University of Nijmegen, Nijmegen, The Netherlands

and

G. W. Webb
Institute for Pure and Applied Sciences, University of California, San Diego, La Jolla, California 92093

(Received 25 January 1978)

de Haas–van Alphen (dHvA) oscillations have been observed in Nb_3Sn in the (110) plane and in V_3Si at two orientations using single crystals of high resistance ratio and magnetic fields in excess of H_{c2}. The dHvA frequency data for Nb_3Sn can be interpreted as a series of nested ellipsoids centered at M, as suggested by a recent high-precision calculation of the Nb_3Sn Fermi surface.

We present the first de Haas–van Alphen (dHvA) measurements of the Fermi surfaces of high-T_c $A15$ structure superconductors, with measurements for both Nb_3Sn and V_3Si. We compare the Nb_3Sn results to a recent band-structure calculation[1] and find good agreement. The upper critical fields, H_{c2}, are ~20 kOe lower than earlier measurements,[2] apparently due to the high-purity single crystals of Nb_3Sn and V_3Si used.

The current high level of interest in $A15$ materials is due to the recent and continuing discoveries of the coexistence of a variety of anomalous normal-state properties[3] at both high and low temperatures, with the highest-T_c materials showing the most puzzling behavior. It is widely felt that the underlying physical features leading to these unusual normal-state properties are also the cause of the high transition temperatures observed in many $A15$-structure materials. A variety of physical models ascribing special features to either the phonon or electron distributions have been invoked to explain the normal-state properties. Our results are a first step in providing a microscopic test of the various electronic models.

Unfortunately, the very properties which make the high-T_c $A15$'s such interesting materials had until now, combined to prevent dHvA measurements of the Fermi surface; the only prior dHvA measurements being the very recent results of Arko, Fisk, and Mueller[4] for Nb_3Sb (T_c ~0.2 K). Magnetothermal oscillations were previously observed in V_3Ge.[5] The main limiting experimental factors are the following. (1) Effective masses are expected to be high because of the intrinsically flat electronic band structure and because of the strong electron-phonon coupling ($\lambda \sim 1.4$ for Nb_3Sn). (2) H_{c2} is large, so that exceptionally high magnetic fields are needed simply to reach the normal state. (3) The materials tend to have high residual (and intrinsic) resistivities[6] so that T_D, the Dingle temperature, would be expected to be large. (4) Some of the most interesting materials undergo a martensitic transformation so that the dHvA signal is suppressed due to interference of oscillations and to phase smearing between tetragonally distorted subdomains.

The Nb_3Sn crystals were grown over a period of four months by closed-tube vapor transport with iodine as the transporting agent. X-ray dif-

fraction on part of the deposit showed only sharp lines of the $A15$ structure with a room-temperature lattice parameter of 5.290 Å. An inductive measurement of the actual dHvA crystal showed a T_c (midpoint) of 17.8 K and a width (10%–90%) of 0.07 K. Resistivity measurements confirm that the samples undergo a martensitic transformation at 51 K. We estimate that $R(300\ \mathrm{K})/R(0\ \mathrm{K}) = 50$ assuming that T^2 is a satisfactory extrapolation function.[6,7] The V_3Si specimen was grown using a floating-molten-zone technique with induction heating in a pure-argon atmosphere. No resistance ratio or T_c measurements were made. However, from the amplitude of the dHvA signals we estimate the purity to be at least comparable to that of Nb_3Sn.

Oriented single-crystal samples were mounted in a spiral-gear-driven rotator. The accuracy with which orientations are known in the (110) plane is estimated to be about 1°.

The experiments were conducted in the 400-kOe "slow-pulsed-field" facility at the University of Amsterdam.[8] The principal advantage of a slow magnetic field pulse is that self-heating and signal-detection problems associated with eddy currents in metallic samples are avoided and mechanical vibrational noise is minimized. All dHvA data were taken in the free-inductive-decay mode from 400 kOe in order to eliminate electrical noise introduced through the current-regulating circuits. The entire system was checked by observing dHvA oscillations in a single crystal of Mg; the results agreed with published values of Mg dHvA frequencies to within 1–3%.

The output of a compensated dHvA pickup coil was differentiated twice, filtered to take out some of the slowly varying voltage resulting from incomplete coil compensation, amplified, and displayed directly on the recorder. A typical recorder tracing is shown in Fig. 1. Since the induced voltage in the dHvA pickup coil is directly proportional to the time frequency of the dHvA oscillations, the usual exponential amplitude increase as H increases will not be observed due to the $1/H$ periodicity of the dHvA oscillations. For low-mass, low-frequency oscillations one may even see an amplitude decrease, which is further accentuated by the dc filter. This decrease in amplitude is clearly evident in Fig. 1.

The dHvA oscillations were analyzed by marking the positions of successive oscillation peaks and making a plot of oscillation number versus $1/H$; the slope of this "number plot" gives the dHvA frequency directly and was generally found to be a good straight line, giving us confidence in our field calibration. Beat structure, while obviously present at some orientations, was difficult to resolve because of the few oscillations

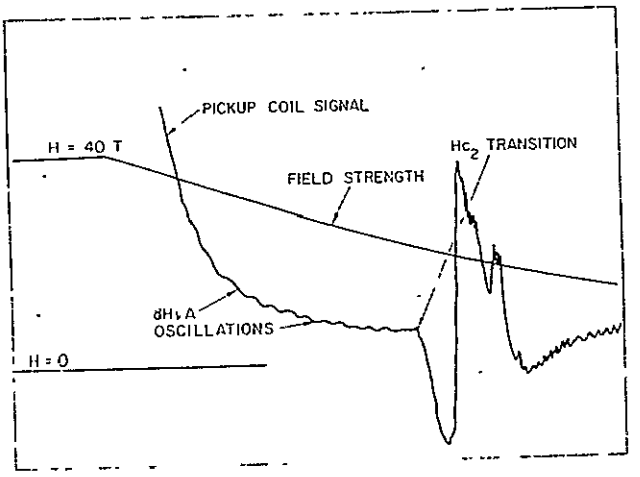

FIG. 1. Dual traces of a typical high-speed chart recording for Nb_3Sn at 75° from [100] showing the decay of a 40-T magnetic field pulse and the simultaneous recording of dHvA oscillations followed by the superconducting transition at H_{c2} vs time (the field decays from 10 T to H_{c2} in about 0.15 sec). The apparent oscillations below H_{c2} are noise generated in the pickup coil in the superconducting state due to eddy currents, flux jumps, etc., and are *not* periodic in $1/H$.

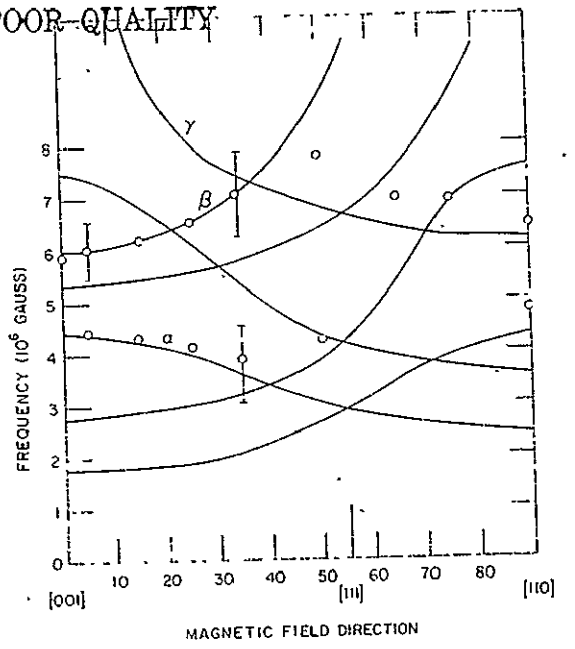

FIG. 2. dHvA frequencies for Nb_3Sn in the (110) plane. The solid circles (with typical error bars) are the experimental results. The solid lines are generated from the Fermi-surface model and band-structure calculation of Ref. 1.

plus the above-mentioned problems with the amplitude dependence. Nevertheless, it is possible to resolve several separate branches in the Nb_3Sn data. Figure 2 displays the dHvA frequencies (open circles) found for Nb_3Sn in the (110) plane, while the limited data for V_3Si are given in Table I. The long cooling time of the magnet (~4 h after each pulse) made it necessary to space data at only 10° intervals. The typical error estimates indicated in Fig. 2 are conservative, based on a maximum possible counting error of one-half oscillation. The reproducibility of the dHvA frequency measurements at a given orientation was a few percent. There was evidence in the raw data for additional dHvA frequencies, both larger and smaller than those presented in Fig. 2. However, the signal-to-noise ratio for these oscillations is barely greater than 1; so they are not included here.

To interpret our results we have used the band calculation of Ref. 1. The calculation is similar to that of Mattheiss[9] (i.e., augmented-plane-wave method used with a *non*-self-consistent overlapping charge-density model, and Slater $\alpha = 1$ exchange) except that non-muffin-tin terms were included, and much greater precision was maintained throughout (i.e., 56 points in $\frac{1}{48}$th of the zone versus Mattheiss's 4, 3-mRy convergence versus 30 mRy, etc.). The solid lines in Fig. 2 are the predicted theoretical frequencies from Ref. 1. The correspondence between the observed frequencies and those labeled α, β, and γ is good. Based on this we conclude that the observed frequencies are consistent with a set of nested ellipsoids at M, similar to the observations in Nb_3Sb[5] and V_3Ge.[6,9] (This conclusion is not reached from the data alone.) Since very low dHvA frequencies are discriminated against in pulsed-field experiments as discussed above, it is reasonable that we do not observe the (low-mass) lowest predicted branches in Fig. 2. Other larger "missing" orbits have too high a mass ($m_{exp}^* \sim 2.4 m_{band}$) to be observed with this relatively insensitive technique. Further, the frequencies bunched near 5×10^6 G are too closely spaced to allow a clear resolution of beats. Within these limitations there is excellent agreement between our data and the predictions of the theory of Ref. 1. While the symmetry of the experimental frequencies is ambiguous, the magnitude is not. Several other band calculations[3,9,10] predict surfaces too large to fit our data, although it was pointed out that the size of small pieces is quite sensitive to the exchange approximation.[10]

TABLE I. dHvA frequencies for V_3Si.

Orientation	Frequency (10^6 G)
[100]	6.24
	4.60
[110]	7.78

We have indirectly and simultaneously measured the anisotropy of the upper critical field H_{c2} for Nb_3Sn at the same 10° intervals. Taking the highest-field point of the normal-to-superconducting transition (H decreasing) as defining H_{c2}, we find that $H_{c2} = 214$ kOe (at $T = 1.5$ K) and is isotropic within the 1% precision of our measurements. (For V_3Si we find $H_{c2} = 216$ kOe at $T = 1.5$ K.) This result is significantly smaller than the earlier (extrapolated) value of 240 kOe at $T = 0$ or $H_{c2} = 235$ kOe at $T = 1.5$ K. We have ruled out that this difference is due to extrinsic effects. Instead, we believe that the lower H_{c2} is intrinsic to the highly perfect (and well annealed) single crystals used. Evidence to support this comes from the fact that a poorer Nb_3Sn specimen, which gave only weak lower-frequency dHvA oscillations, had a higher critical field ($H_{c2} \sim 230$ kOe along [100]) and also displayed some slight anisotropy of H_{c2} (slightly lower values elsewhere), consistent with literature values.[2]

A significant concern for future dHvA experiments on Nb_3Sn may turn out to be the effect of thermally cycling a single crystal through the structural transformation. Repeated thermal cycling decreased the dHvA amplitudes by at least a factor of 2. These were restored by annealing at 700°C for five days. Our data do not yet allow us to determine which factor (high T_D, phase smearing, changes in electronic structure) is primarily responsible for the signal degradation. The change in the lattice parameter accompanying the transformation is only of order 1% so that a major change in the band structure is not expected. It does seem, however, that it may be possible to use the dHvA effect as a detailed probe of the electronic consequences of the A15 structural transformation and defect formation.

We acknowledge the help provided by Dr. Sven Hornfeldt in connection with the sample rotator design, and by Mr. Weizenbeek in connection with data logging. This work was supported by the U. S. Department of Energy, the National

Science Foundation, the Stitching voor Fundamenteel Onderzoek der Materie (The Netherlands), and the National Aeronautics and Space Administration.

[1]A. T. van Kessel, H. W. Myron, and F. M. Mueller, to be published.

[2]S. Foner and E. J. McNiff, Jr., Phys. Lett. 58A, 318 (1976).

[3]For a review see M. Weger and I. B. Goldberg, in *Solid State Physics*, edited by H. Ehrenreich, F. Seitz, and D. Turnbull (Academic, New York, 1973), Vol. 28; L. R. Testardi, in *Physical Acoustics*, edited by W. P. Mason and R. N. Thurston (Academic, New York, 1973), Vol. 10.

[4]A. J. Arko, Z. Fisk, and F. M. Mueller, Phys. Rev. B 16, 1387 (1977).

[5]J. E. Graebner and J. E. Kunzler, J. Low Temp. Phys. 1, 443 (1969).

[6]See, for example, Z. Fisk and G. W. Webb, Phys. Rev. Lett. 36, 1084 (1976); and D. W. Woodard and G. D. Cody, Phys. Rev. 136, A166 (1964).

[7]G. W. Webb, Z. Fisk, J. J. Engelhardt, and S. D. Bader, Phys. Rev. B 15, 2624 (1977).

[8]R. Gersdorf, F. A. Muller, and L. W. Roeland, Rev. Sci. Instrum. 36, 1100 (1965).

[9]L. F. Mattheiss, Phys. Rev. B 12, 2161 (1975).

[10]B. Klein, L. Boyer, D. Papaconstantopoulos, and L. Mattheiss, unpublished and private communication.

JOURNAL DE PHYSIQUE

Colloque C6, supplément au n° 8, Tome 39, août 1978, page C6-1385

FERMI SURFACE AND dHvA EFFECT IN THE NORMAL STATE OF HIGH T_c A-15 SUPERCONDUCTORS +

A.J. Arko[+], D.H. Lowndes[†], A.T. Van Kessel[++], H.W. Myron[++], F.M. Mueller[++], F.A. Muller[**], L.W. Roeland[**], J. Wolfrat[**], and G.W. Webb[††]

[+]*Materials Science Division, Argonne National Laboratory, Argonne, IL. 60439, U.S.A.*
[†]*Department of Physics, University of Oregon, Eugene, OR 97403, U.S.A., and Physics Laboratory, University of Nijmegen, Nijmegen, The Netherlands*
[++]*Physics Laboratory, University of Nijmegen, Nijmegen, The Netherlands*
[**]*Natuurkundig Laboratorium, University of Amsterdam, Amsterdam, The Netherlands*
[††]*Institute for Pure and Applied Sciences, University of California, San Diego, La Jolla, CA 92093, U.S.A.*

Résumé.- La surface de Fermi de Nb_3Sn a été déterminée par des calculs de bande de type APW. Des oscillations de Haas-van Alphen (dHvA) ont été observées dans Nb_3Sn et dans V_3Si en accord avec la surface de Fermi calculée. Pour ces deux composés, à l'état normal des oscillations dHvA ont été mesurées avec des monocristaux ayant un haut rapport de résistivité plongés dans des champs magnétiques allant jusqu'à 400 kOe et les nouveaux details de la surface de Fermi ont été mis en évidence et en particulier une structure ellipsoïdale osculatrice autour de M et une grande structure cubique autour de Γ.

Abstract.- The Fermi surface of Nb_3Sn has been derived form an APW band calculation. de Haas-van Alphen (dHvA) oscillations have been observed in Nb_3Sn and V_3Si which give a consistent FS description. Using single crystals of high resistance ratio's and magnetic fields up to 400 kOe, dHvA oscillations have been seen in the normal state for both specimens. New features of the Fermi surface include osculated ellipsoidal structure around M, and a large cubical structure around Γ.

The current high level of interest in A-15 materials is due to the recent continuing discoveries of the coexistence of a variety of anomalous normal state properties /1/ at both high and low temperatures, with the highest T_c materials showing the most puzzling behavior. It is widely felt that the underlying physical features leading to these unusual normal state properties are also the cause of high transition temperatures observed in many A-15 structure materials. A variety of physical models ascribing special features to either the phonon or electron distributions have been invoked to explain the normal state properties. Detailed knowledge of the band structure is a necessary precursor and underpinning to the inclusion of the electron-phonon and electron-electron couplings and hence to the theory of superconductivity in these materials. The only prior dHvA measurements on an A-15 are the recent results of Arko et al. /2/ for Nb_3Sb ($T_c \sim 0.2$ K). Magnetothermal oscillations were previously observed /3/ in V_3Ge ($T_c \sim 6$ K). Recently (some of us) have reported /4/ on the global energy structure of Nb_3Sn. Here we now report on band properties close to E_F — the derived Fermi surface. Briefly the calculated extremal cross-sectional areas agree within 3 to 5% with the dHvA data presented here for sheets near M. In addition we find a very large-massed ($m^* = 2.3$) cubical "box-like" structure near Γ which we identify with breaks in the derivatives of the positron annihilation data of Samoilov and Weger /5/ on the isoelectronic material V_3Si.

Unfortunately, the very forces which make the high T_c A-15's such interesting materials had, until now, combined to prevent dHvA measurements of the Fermi surface, the only prior dHvA measurements being the very recent results for Nb_3Sb /2/. The four main limiting experimental factors are :

1) Cyclotron effective masses are expected to be high due to the intrinsically flat electronic band structure and to the strong electron-phonon coupling ($\lambda \simeq 1.4$ for Nb_3Sn) ;

2) H_{c2} is large, so that exceptionally high magnetic fields are needed, simply to reach the normal state ;

3) Single crystals tend to grow nonstoichiometrically so that T_D, the Dingle temperature, would be expected to be large. The A-15's tendency toward intrinsic defect formation is presumably also accompanied by high dHvA Dingle temperatures ;

4) Crystals undergo martensitic transformation in cooling from room to helium temperature, so that suppression of the dHvA signal due to interference of oscillations and to phase smearing between tetra-

+ Work supported by the U.S. Department of Energy, the National Science Foundation (USA), the Stichting voor Fundamenteel Onderzoek der Materie (The Netherlands) and NASA (U.S.A)

gonally distorted subdomains is expected. Both phase smearing and scattering (Dingle temperature) contribute to an exponential attenuation of the dHvA amplitude, with phase smearing becoming more pronounced as the dHvA frequency increases.

The Nb_3Sn crystals were grown over a period of four months by closed tube vapor transport with iodine as the transporting agent. An inductive measurement of the actual dHvA crystal showed a T_c of 17.8 K and a width (10 % - 90 %) of 0.07 K. Resistivity measurements confirm that the samples undergo a martensitic transformation at 51 K. Assuming an approximate extrapolation function /6/ we estimate R (300 K) / R (0 K) = 50 and R (0 K) = 1.5 μΩcm /7/. From this residual resistivity we estimate an electron mean free path of about 500 Å and $\omega_c\tau \geq 1$ in magnetic fields above 230 kOe, where ω_c is the cyclotron frequency and τ is a mean scattering time. This consideration is suggestive of the scattering time being high enough to see the dHvA effect.

The V_3Si specimen was grown using a floating molten zone technique with induction heating in a pure argon atmosphere. The zone was passed along the rod (obtained by melting the consistent metals in a silver boat) at the rate of ≈ 2 cm/h. A multigrained sample was obtained which had a large central grain the length of the sample (≈ 1/8" diam.). No resistance ratio or T_c measurements were made. However, it is known that V_3Si is less susceptible than Nb_3Sn to the A-15 tendency toward defect formation, while the amplitude of the dHvA signals makes it clear that the total scattering rate in V_3Si must be at least comparable to that of Nb_3Sn. The quality of both the Nb_3Sn and V_3Si crystals was very good, as indicated by examination of the room temperature diffraction spots in Laue back-reflection x-ray pictures. Both the Nb_3Sn and V_3Si crystals were cut by spark erosion into specimens ≈ 1 mm^3 and surface damage etched away. Oriented single crystal samples were mounted in a spiral gear driven rotator with the magnetic field within about 1° of a (110) plane ; the accuracy with which orientations are known in the (110) plane is also estimated to be about 1°.

The experiments were conducted at the University of Amsterdam's 400 kOe "slow pulsed field" facility using the magnet in the free inductive decay mode to minimize noise /8/. The output of a compensated dHvA pickup coil was differentiated twice, filtered to take out some of the dc voltage resulting from incomplete coil compensation, amplified and displayed directly on the recorder. A typical recorder tracing is shown in figure 1.

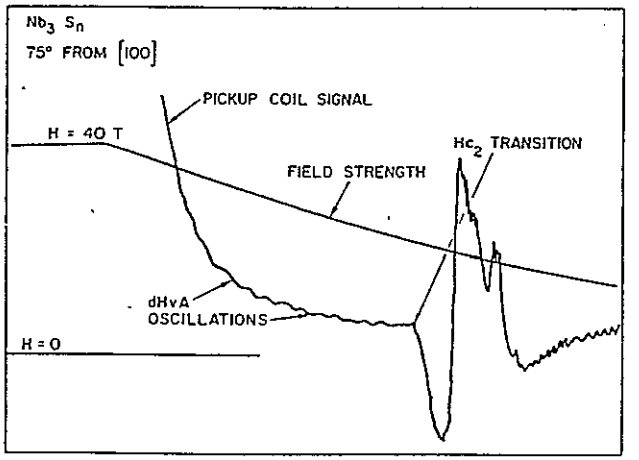

Fig. 1 : Dual traces of a typical high speed chart recording for Nb_3Sn, showing the decay of a 40 T magnetic field pulse and the simultaneous recording of dHvA oscillations followed by the superconducting transition at H_{c_2} versus time. The apparent oscillations below H_{c_2} are noise generated in the pickup coil due to eddy currents, flux jumps, etc.., and not periodic in 1/H.

The dHvA oscillations were analyzed by marking the positions of successive oscillation peaks and making a plot of oscillation number versus 1/H ; the slope of this "number plot" gives the dHvA frequency directly and was generally found to be a good straight line. Beat structure, while obviously present at some orientations, was difficult to resolve because of the few oscillations. Nevertheless, it is possible to resolve several branches in the Nb_3Sn data. Figure 2 displays the dHvA frequencies (open circles) found for Nb_3Sn in the (110) plane, while the limited data for V_3Si are given in Table I. The typical error estimates indicated in figure 2 are conservative, based on a maximum possible counting error of one-half oscillation.

Table I

dHvA Frequencies for V_3Si

Orientation	Frequency (10^6 gauss)
[100]	6.24
	4.60
[110]	7.78

Until recently the intrinsic resolution of band theoretical calculations for materials as com-

plex as the A-15's was no better than about 4,000 K /1,9/ precluding direct theoretical exploration of electronically-driven models for the many interesting A-15 anomalies. However, we will interpret our experimental results here by comparing them with the Fermi surface predicted by a new high precision energy band model for Nb_3Sn, for which the intrinsic resolution is less than 500 K /4/.

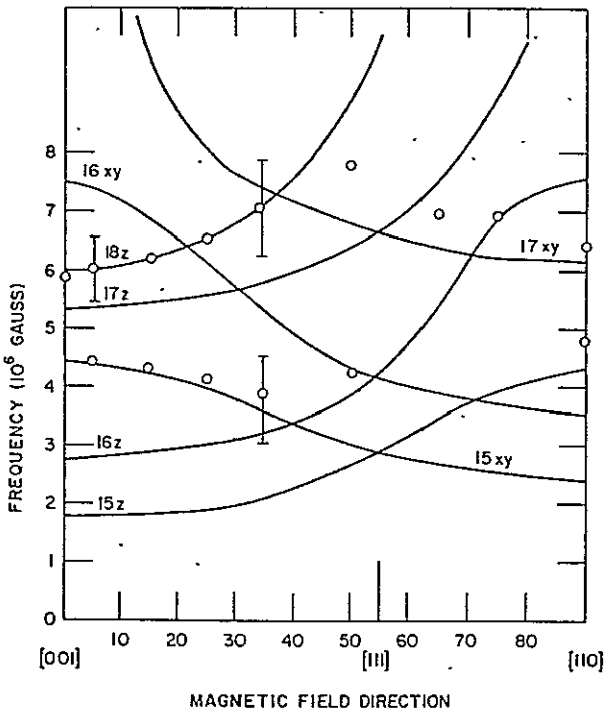

Fig. 2 : dHvA frequencies for Nb_3Sn in the (110) plane. The solid circles (and typical error bars) are the experimental results. Accuracy of orientation in the (110) plane is 1°. The frequencies at a given orientation are reproducible to within a few %. The solid lines are generated from the Fermi surface model and band structure calculation of reference /4/

In figure 3 we present the Fermi surface of Nb_3Sn (intersecting bands 15-21) in the principal symmetry planes. The Fermi energy was determined exactly from the density of states /4/ and no adjustable parameters were used. Because of the sensitivity of figure 3 to small energy shifts (especially bands 19 and 20) we have used the (larger than 300th order) APW secular matrix itself as an interpolation scheme to make the plot.

Two features are noteworthy compared to the previous V_3Si isoelectric Fermi surface of Mattheiss /9/ :

1) the greater confluence of osculated structure at M ;

2) the flat "box-like" structures centered at Γ.

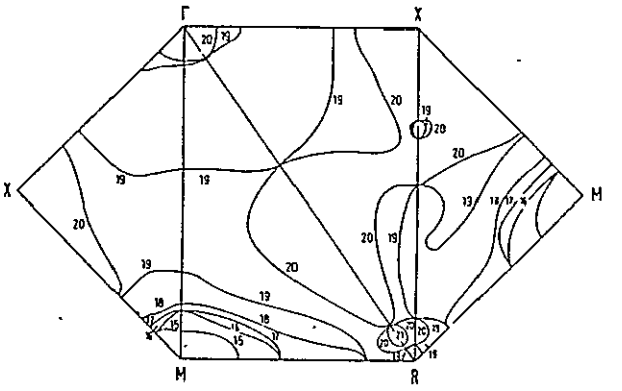

Fig. 3 : The Fermi surface of Nb_3Sn. The band indexing follows reference /4/. Note that the positions of the labels follows the filling of $\vec{k}$ space volumes so that band 20 near Γ is an electron piece and band 15 near M is a hole piece.

Globally the Nb_3Sn band structure was the same as that of Mattheiss. Making a microscopic comparison near E_F between his /9/ figure 6(d) and figure 1 of reference /4/, we find that the main result is that Γ_{12} has "dropped" by about 30 mRy relative sets of levels at M - a result easily understood in that we have included an extra (negative) potential inside the muffin-tin-spheres (primarily Nb-along-the-"chains") relative to Mattheiss. Hence the d-like Nb bonding state Γ_{12} near E_F - which is maximally sensitive to such effects - "drops" relative to the insensitive levels at M. Since the Fermi level follows the heavy massed Γ_{12} state, the "light" massed M-centered hole-like levels seen in figure 3 "pop-up" through E_F. The structure near R also has a light mass. We have fitted the values of the "light-massed" bands 15-19 at 10 points near M to the lowest 7 M-harmonics by a least squares procedure :

$$E_n(\underline{k}) = \Sigma\, C^n_{\ell mp}\, x^\ell y^m z^p \qquad (1)$$

where $E_n(\underline{k})$ is the energy of band n at point $\underline{k}$, the C's are the expansion coefficients and x, y, z are the components of the k-vector difference from M, in atomic units. All terms through quartic (i.e. z^4) were used. These were used to obtain the areas and masses, $m^* = (1/\pi)dA/dE$ listed in table II. In general, the correspondence between the observed and calculated dHvA frequencies (figure 2 and table II) is good. (The experimental labeling and identification was based on the angular dependence of the areas). We have listed in table II the masses for the M-centered pieces as a guide to understanding the experimental data. Very low dHvA frequencies we-

re discriminated against in the pulsed field experiments, both because their period in H was too long and for other experimental reasons /10/. Most other M-centered "missing" orbits probably had too high a mass to be observed ($m^*_{exp} \gtrsim 2.4\ m_{band}$), although it is surprising that 17(z) at [110] were missing. In view of the difficulty of the measurements and calculations the overall agreement is satisfactory and we conclude that the dHvA oscillations we have seen are consistent with a series of oscilated ellipsoids at M. Guided by Mattheiss'band calculations /9/, both Graebner and Kunzler /3/ (for V_3Ge) and Arko, Fisk and Mueller /2/ (for Nb_3Sb) have also interpreted their data in terms of M-centered structures, although those interpretations required rigid shifting of E_F upward.

Table II

Areas and masses in the [001] and [110] directions in atomic units.
The convention of M labeling is as in figure 2.

Direction	[001]			[110]		
Symmetry	A_{exp} [a] (× 100)	A_{theory} (× 100)	m^*_{theory} [b]	A_{exp} [a] (× 100)	A_{theory} (× 100)	m^*_{theory} [b]
M-centered orbits						
15(z)		0.47	0.23		1.16	0.42
16(z)		0.74	0.64		2.02	0.97
17(z)		1.43	0.43			
18(z)	1.58	1.61	0.46			
15(x,y)	1.12	1.17	0.35		0.65	0.32
16(x,y)		2.01	1.03		0.99	0.77
17(x,y)				1.59	1.66	0.49
Γ-centered orbits						
19		13.14	2.13 ± 0.05		13.66	2.90 ± 0.15

a) experimental data.

b) m^*_{theory} should be multiplied by $(1+\lambda) \sim 2.4$ to obtain experimental masses.

For the Γ-centered sheet, we have found it impossible to make a satisfactory expansion of the 19th band energy structure in a few cubic harmonics /11/, analogous to equation (1). The areas and masses listed in table II for the Γ-centered sheet were derived numerically from $\vec{k}$ vectors found from the APW secular matrix. The errors of the two 19th band masses are relatively large because they were found by numerical differentiation. (The effective energies used were spaced 0.5 mRy apart.) We have given M-centered and Γ-centered masses also to stimulate measurements of the cyclotron mass. The mass of the Γ-centered piece normal to [001] is rather constant for different values of k_z. Hence most of that Fermi surface sheet should contribute at a single value of m^*. This should help to make the rather high value of cyclotron mass of about 5 observable. Although our predicted Fermi surface is somewhat complicated, there are clear open and closed directions. We ask that high field magneto-resistance experiments be considered as a further test of our Fermi surface topology.

We now focus on an unexpected feature of figure 3 : the two cubical "box-like" structures of band 20 and 19 centered at Γ and intersecting the Γ to X ([100]) line at 0.15 and 0.64 π/a units respectively, and the Γ to M ([110]) line at 0.15 and 0.62 π/a units, respectively. These features were invariant to slight shifts (± 3 mRy) of E_F, although the exact intersection distances varied slightly with E_F. Recently Samoilov and Weger have reported /5/ positron annihilation experiments in iso-electronic V_3Si in the [100] direction, and we have enhanced the sensitivity of their data to Fermi surface effects by means of a novel "folding" technique. Although the resolution of their experiment was limited to 0.5 milliradians (or 0.196 π/a units), they find (their figure 2) derivative structure with 3 peaks along [100] at 0.185, 0.635 and 0.844 π/a units. Clearly there is good agreement between the flat band 20 and 19 intersections of [100] and their first two peaks. Band 20 is a possible candidate for their third peak structure - particularly the flat structure centered around X in confluence with the multiple structure at M. But these third peak identifications are tentative. We have assumed an invariance between the detailed band structure shape near E_F of V_3Si and Nb_3Sn. Comparing figures 6a-6d of Mattheiss /9/ there is a close family ressemblance - but microscopically our Nb_3Sn bands are more like his V_3Si bands than his Nb_3Sn bands. Samoilov and Weger have interpreted /5/ their data in terms of the independent band model /1/ whose chief difference near E_F from our model is that they find that E_F intersects the $\Gamma_{25'}$ levels and that their Γ_{12} levels are above E_F. Our results support Samoilov and Weger's main conclusion of the importance of planar Fermi surface structures along [100]

in A-15 materials although our interpretation and wave functions near E_F is different from theirs. (If we artificially modify the potential to place E_F at $\Gamma_{25'}$, we loose agreement with the M-centered dHvA data.) Weger has suggested /12/ a high magnetic field NMR experiment as a definitive test of Γ_{12} vs. $\Gamma_{25'}$. We ask that experimentalists also consider further high resolution positron annihilation work in A-15 materials along other high symmetry directions as a test of band models. We predict that there should be a smaller but similar break along [110] - we believe that the Samoilov-Weger model would predict smooth behavior in that direction.

The correspondance between the observed frequencies and those labeled 15(xy), 18z and 17(xy) is good. We conclude that the observed frequencies are consistent with a set of nested ellipsoids at M, similar to observations in Nb_3Sb /2/ and V_3Ge /3/. The very low dHvA frequencies are discriminated against in pulsed field experiments, it is reasonable that we do not observe the lowest predicted branches of figure 2.

Finally, our present data clearly do not allow us to determine whether the disappearance of the higher frequency oscillations as a result of thermal cycling was due to the (progressive) disappearance of a piece of Fermi surface, accompanying the structural transformation, or simply due to an increase in Dingle temperature (electronic scattering rate) due to strain. The change in the lattice parameter accompanying the transformation is only of order 1 % so that a major change in the band structure is not expected. One would expect the degeneracy of the branches to be lifted, but our data are not sufficiently accurate to determine any minor splittings in the dHvA frequency branches. However, it does seem clear from our measurements that the effects of the martensitic transformation are reversible, and that it will be possible to use the dHvA effect as a detailed probe, in k-space, of the electronic consequences of the A-15 structural transformation.

We would like to acknowledge the help provided by Dr. Sven Hornfeldt in connection with the sample rotator design, by Mr. Weizenbeek in connection with data logging, and the generous support provided to one of us (DHL) by the University of Nijmegen during the time these experiments were being conducted.

References

/1/ For a review see : Weger, M., and Goldberg, I.B., in Solid State Physics, H. Ehrenreich and D. Turnbull, eds. (Academic Press, N.Y.), 1973, vol. 28 ; Testardi, L.R. in Physical Accoustics, W.P. Mason and R.N. Thurston, eds. (Academic Press, N.Y.), 1973, vol. 10

/2/ Arko, A.J., Fisk, Z., and Mueller, F.M., Phys. Rev. B 16 (1977) 1387

/3/ Graebner, J.E. and Kunzler, J.E., J. Low Temp. Phys. 1 (1969) 443

/4/ Kessel van, A.T., Myron, H.W., Mueller, F.M. (these proceedings)

/5/ Samoilov, S. and Weger, M., Solid State Commun. 24 (1977) 821

/6/ Webb, G.W., Fisk, Z., Engelhardt, J.J. and Bader, S.D., Phys. Rev. B 15 (1977) 2624

/7/ Woodard, D.W. and Cody, G.D., Phys. Rev. 136 (1964) A166

/8/ Gesdorf, R., Muller, F.A., and Roeland, L.W., Rev. Sci. Instrum. 36 (1965) 1100.

/9/ Mattheiss, L.F., Phys. Rev. B 12 (1975) 2161

/10/ Arko, A.J., Lowndes, D.H., Muller, F.A., Roeland, L.W., Wolfrat, J.W., van Kessel, A.T., Myron, H.W., Mueller, F.M., and Webb, G., Phys. Rev. Lett. 40 (1978) 1590

/11/ Lage vd, F.C., and Bethe, H.A., Phys. Rev. 71 (1974) 612

/12/ Weger, M. (private communication)